Numerical Simulation of Environmental Flow over Urban Landscape for Applications to Renewable Energy

by

Xiaoyan Ying

A Thesis Presented in Partial Fulfillment
of the Requirements for the Degree
Master of Science

Approved April 2015 by the
Graduate Supervisory Committee:

Huei-Ping Huang, Chair
Yulia Peet
Marcus Herrmann

ARIZONA STATE UNIVERSITY

May 2015

ABSTRACT

Development of renewable energy solutions has become a major interest among environmental organizations and governments around the world due to an increase in energy consumption and global warming. One fast growing renewable energy solution is the application of wind energy in cities. To qualitative and quantitative predict wind turbine performance in urban areas, CFD simulation is performed on real-life urban geometry and wind velocity profiles are evaluated. Two geometries in Arizona is selected in this thesis to demonstrate the influence of building heights; one of the simulation models, ASU campus, is relatively low rise and without significant tall buildings; the other model, the downtown phoenix model, are high-rise and with greater building height difference. The content of this thesis focuses on using RANS computational fluid dynamics approach to simulate wind acceleration phenomenon in two complex geometries, ASU campus and Phoenix downtown model. Additionally, acceleration ratio and locations are predicted, the results are then used to calculate the best location for small wind turbine installments.

DEDICATION

To my parents,

Ji Xue and Xiaoping Ying

ACKNOWLEDGEMENTS

I take this opportunity to thank Dr. Huei-Ping Huang, my advisor and mentor for his support and guidance throughout this project. His valuable feedback and encouragement kept pushing me forward and complete this project in time.

I also thank Dr. Yulia Peet and Dr. Marcus Herrmann for having agreed to be on my thesis committee.

I am grateful for the encouragement and support from my mother, father, family and friends, I would not be able to do this without them.

Lastly, I would like to thank my grandparents for their unconditional love and support, for which they will always be missed.

TABLE OF CONTENTS

Chapter Page

Chapter Page

LIST OF TABLES

Figure Page

LIST OF FIGURES

Figure Page

Figure Page

Figure Page

Figure Page

Figure Page

CHAPTER 1

INTRODUCTION AND METHODOLOGY

1. Introduction

Development of renewable energy solutions has become a major interest among environmental organizations and governments around the world due to an increase in energy consumption and global warming. A combination of renewable energy solutions will be required in the near future to meet our overall goals, renewable energy solutions such as wind, solar and hydropower will all play a part when dealing with the global energy crisis. Aside from these varies technologies been involved, multiple applications and size scales are also considered to fit in with different requirements.

One renewable energy solution in fast development is the application of wind energy in cities. While large-scale wind turbines have been widely used for years and currently playing a crucial part in energy generation in offshore and remote areas, more attention have been raised on the application of smaller wind turbines.

Although there is a growing interest in these small roof-mounted turbines, the knowledge of its mounting site is very limited. Due to the fact the performance of these turbines is very site sensitive, surroundings of the mounting location plays a vital part in the power generation ratio. This thesis will support this growing level of interest by providing individuals and small enterprises with the knowledge necessary to make decisions on turbine mounting locations.

Conceptual Framework

1.2.1 Wind energy and wind turbines in urban area

As renewable energy generation technologies have gain a fast development over the past decades, general public have gradually coming to aware that a combination of renewable energy solutions will be required in the near future to meet our overall goals, renewable energy

solutions such as wind, solar and hydro power will all play a part when dealing with the global energy crisis, while turbines and solar modules are the most widely applied technology among them. It is commonly accepted that wind turbines are effective and efficient at large scale conditions, especially off shore cases where wind are strong enough to produce large amount of power. On the other hand, when coming to small scales, especially considering the complicate structure of modern cities, solar panels are more favored over wind turbines. The reason why wind turbines are not as common installed as solar systems in cities is because a lot of turbines have high cut-off velocities, which make them unable to work unless wind speed reaches that cut-off value. Moreover, the wind velocity in urban environment is relatively low due to the numerous buildings acting as wind blocks.

Although solar power systems have developed quickly across the years, there are some obvious drawbacks, for example, sun power is not enough to generate reasonable amount of energy in some seasons (Bruno Burger 2014), and the fact that solar panels cannot work when there is no sunlight. Thus makes it better preferred to combine these two energy solutions together.

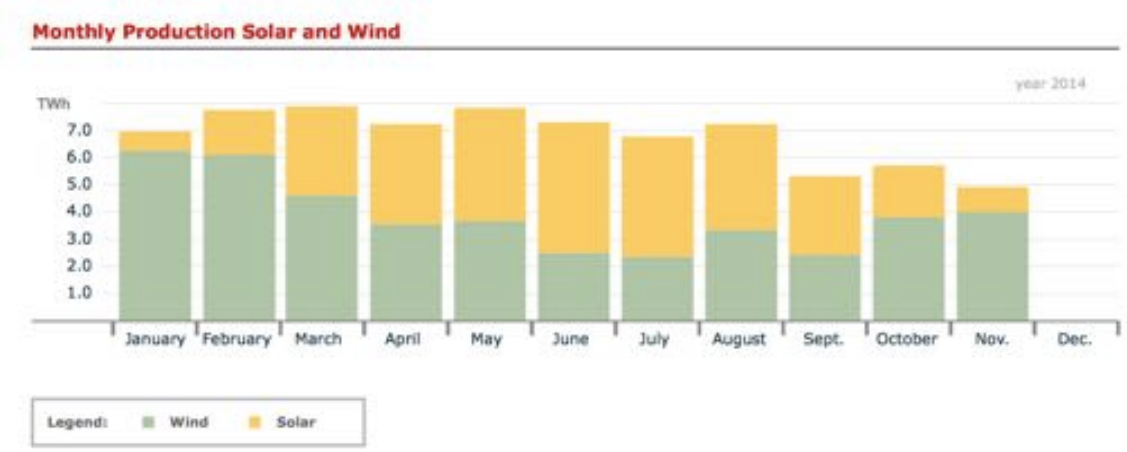

Figure 1.1: Wind and solar energy generation comparison in twelve months. The chart is from Conference Electricity Production from Solar and Wind in Germany, 2014.

For applications in urban environment, instead of choosing wind turbines with higher

capacity and energy production rate, smaller turbines that generate power at lower wind speed would be a better choice. Resent years have seen a boom in the small wind turbine industry; a lot of companies are working on smaller wind turbines for application in urban environment and other low-wind velocity locations in need of power, leisure boats for example. Cheaper small wind turbines in the market are often low quality and heavier, these turbines performs poorly at low wind speed and are usually less efficient. Ideally, a small wind turbine for application in cities should start spinning at as low as 1 m/s wind velocity.

1.2.2 Small wind turbine installation

Small wind turbines are very site specific (Michael Boxwell 2011), even mild turbulence structures in urban environment can greatly affect efficiency of the turbines, thus making site survey before wind turbine installment vitally important. To gain sufficient velocity for power generation, most wind turbines installed in cities a couple of years ago are mounted 8-10 m above ground as in Fig 1.2. In those cases, it is impossible to put this kind of buildings on building tops as turbine pole at such height can cause significant amount of vibration on the building structures.

Figure 1.2: Small wind turbine with high-rise pole mounted behind a tall tree. The picture is a less-than-ideal wind turbine installation example

This kind of mounting method is not preferable as a turbine at this size can be quite

expensive and because of the multiple threes and building structures surrounding the turbine in city areas, these turbines are often less productive than expected.

A better idea is to mount turbines with smaller diameters on roof-tops, these turbines can goes to as low as a thousand dollars or so, which makes it more preferable by individuals. However, at the early stage of this kind of installing these small turbines, people did not realize the importance of site survey, and a lot of turbines are installed on low-rise buildings with high buildings and trees around, these blocks can form low velocity vortex on the roofs where the wind turbines are installed, thus making the turbines unable to work efficiently.

Roof-turbine wrong site 1 Roof-turbine wrong site 2 Roof-turbine wrong site 3

Figure 1.3: Wind turbines were installed near wall, on low-rise building and in built area. These are three poorly chosen wind turbine installation site examples.

As can be observed form the pictures above, in the first case, a tiny wind turbine was installed near a high wall, the second case shows multiple turbines been installed on a relatively low building with tall trees and high buildings around, this picture is taken in ASU campus. The third one shows a wind turbine mounted on the corner of a roof with trees and other buildings surrounding it. In all cases above, wind turbines are adversely affected from turbulence from either the trees or the higher structures around.

It can be safely concluded from the poor location surveys above that that it is important to know the wind velocity distribution surrounding installation location before moving on to the next step. One way to get the local velocity on rooftops is by in-situ measurement, which gives a trustworthy result but less operable and very time consuming at the same time. CFD simulations have been widely used by researchers to assess the wind performance in urban area,

some of them use commercial software for simulations, their results and experiences are very useful considering the great potential of accurately predicting wind behavior with commercial soft wares. For individuals and small enterprises, instructions on performing turbulence behavior simulations would be very helpful as commercial software are easier to have access to.

1.3 Research methodology

The aim of this research is to identify the effect of inlet wind velocity on the wind acceleration value and location in realistic geometry models, to achieve this aim the following methodology is adopted.

1.3.1 Research methodologies for assessing wind flow around buildings

Varies methods have been adopted by previous researchers to assesse wind flow around buildings, among them are anemometers measurements, wind tunnel experiments and computational fluid dynamics (Abohela 2012). For mounting site selection, a combination of two or more methods would be able to give a convincing result. In this paper, CFD simulations with commercial software on real-life geometries are conducted. The paper takes a look on qualitative results by predicting the wind velocity acceleration structure on building tops and quantitative results by compare wind velocity on building tops with wind speed at inlet. The qualitative results give guidance for wind turbine installation locations and quantitative result tells how much the wind has accelerated on building tops.

1.3.2 Previous Research and Selection of geometry

One important usage for CFD simulations is on real life urban geometries. Many previous researchers have performed CFD simulation on city models. Bazrafshan, J *et al.* (2012) conducted simulations through CFD method and k-ε turbulence model was utilized to analyze flow fluctuations in Navier-Stokes equations. Blocken, B., and J. Persoon (2009) used three-dimensional steady Reynolds-averaged Navier–Stokes (RANS) Computational Fluid Dynamics (CFD) simulations in combination with the new Dutch wind nuisance standard to assess

pedestrian wind comfort around a large football stadium in Amsterdam, before and after the addition of new high-rise buildings. The study focused on the elevated circulation deck and the surrounding streets and squares and CFD validation was performed by comparison of the simulated mean wind speed at the deck with full-scale measurements. Y. Jie *et al.* (2014) use a combination of GIS and CFD method on both the urban and the residential neighborhood scale to explore the relationship between the urban morphology and the urban wind environment.

In this thesis, two geometries in Arizona is selected, to demonstrate the influence of building heights; one of the simulation models, ASU campus, is relatively low rise and without significant tall buildings; the other model, the downtown phoenix model, are high-rise and with greater building height difference.

Both cases are tested in Ansys fluent with atmospheric boundary layer profile at inlet and results are evaluated with methods mentioned above.

Chapter 2

TURBULENCE MODEL AND WIND ACCELERATION OVER BUILDINGS

2.1 Introduction

CFD simulation on urban geometry has been performed by a lot of researchers under various methods in recent years. As mentioned earlier, one of the many applications of ABL simulations is to decide the feasibility of installing wind turbines on rooftops. However, in order to specify the acceleration ratio and locations, an investigation on the wind resources and local wind behavior over building tops is required.

This chapter is divided into three parts mainly; the first section will be on the define of Atmospheric Boundary Layers and parameter calculations; the second section will briefly discuss the acceleration phenomenon to give a quick view of how and why turbulence structure on building tops interest researchers; the third chapter focuses mainly on comparison of characterization of urban wind under multiple turbulence models; while the last section takes a look at the effect of roof turbine on the wind acceleration location and value.

2.2 Atmospheric boundary layer in urban area

2.2.1 Definition of the ABL profile

The wind generated by global and local wind mechanisms interact with natural and manmade features of the Earth's surface. At the bottom of atmospheric domain the wind speed remains zero, however at higher altitude, where wind is more determined by resultant of a pressure gradient force and Coriolis force, the geostrophic wind speed is essentially unaffected by the surface features. The region between the ground surface and geostrophic boundary layer is commonly defined as Atmospheric Boundary Layer. Sheer forces at the boundary between the surface and the air generates turbulence, thus enhances mixing and dissipates the wind's energy at the surface (Ai, Z.T. and C.M. Mak 2015). As greater surface roughness will generate sheer force that causes more turbulence, we can say that surface features of ground would have a

big impact on the surface boundary layer. To characterizes surface roughness, Roughness Length, z_0 is defined (Lettau, 1969) in Figure 2.1:

$$z_0 = \frac{1}{2} \cdot \frac{h \cdot S}{A_h}$$

Where parameters h = height of roughness element, S = roughness element cross-sectional area facing wind, A_h = average horizontal area available to each roughness element.

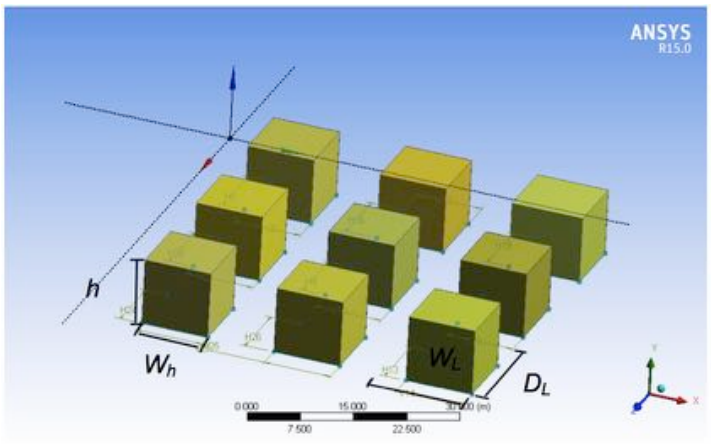

Figure 2.1: Rural area geometry models for demonstration of parameters in roughness height calculation

For geometry of interest like ASU campus, z_0 can be calculate from equations below:

W_L = 30 m, D_L = 30 m, A_H =W_L * D_L =900 m^2;

W_H = 20 m, h = 7 m^2, S = h * W_H = 140 m^2;

From that, we have:

$$z_0 = \frac{1}{2} \times \frac{7\ m \times 140\ m^2}{900\ m^2} = 0.54\ m$$

A widely used way of characterizing ABL in numerical simulations is developed by Prandtl Prandtl (Anderson, J.D. 1997) by representing dependence of wind speed on height, V_z, in a turbulent boundary layer:

$$V_z = \frac{V^*}{K} \ln\left(\frac{z}{z_0}\right)$$

Where z = height above the ground, z_0 = roughness length, V^* = friction velocity, k = Karman constant of the airflow in the boundary layer. One thing to notice is that the utility of the equation is limited as V^* and k are difficult to determine accurately.

As most urban wind speeds from meteorological stations are measured at certain height above ground, calculating wind speed at different heights based on measured wind velocity at a reference height turns out to be very useful in predicting ABL profiles.

$$V(z) = V_r(z_r) \frac{\ln\left(\frac{z}{z_0}\right)}{\ln\left(\frac{z_r}{z_0}\right)}$$

Where z_0 = roughness length, a physical dimension that characterizes the scale of surface roughness, z_r = reference height, $V_r(z_r)$ = measured velocity at the reference height.

The approximate wind profile can be calculated according to the equation above with velocity at reference height and roughness length.

2.2.2 Wind velocity Weibull distribution

In order to calculate the likely power output from a given wind turbine it is necessary to understand the wind in the planned turbine location. Wind velocity varies constantly under nature environment. In order to successfully predict wind turbine's production it is necessary to know exactly how often the wind blows how strongly. In most cases, wind velocity is measured with an anemometer mounted 10 m above ground and the average wind speed is recorded every 10 min (Kauffman *et al.* 2013). The observed data is then sorted into classes of 1 m/s each. The energy contained in the wind at a certain site can be expressed by the frequency distribution equation below.

$$f(v) = \frac{k}{A}\left(\frac{v}{A}\right)^{k-1} exp\left(-\left(\frac{v}{A}\right)^{k}\right)$$

Where A = the Weibull scale parameter in m/s; a measure for the characteristic wind speed of the distribution. A is proportional to the mean wind speed.

k = the Weibull form parameter. Which specifies the shape of a Weibull distribution and takes on a value of between 1 and 3. A small value for k signifies very variable winds, while constant winds are characterized by a larger k (Bhattacharya *et al. 2009*).

The Weibull distribution is considered as a good approximation for the wind speed distribution in continues time period. Based on observation data from Tempe Town Lake Weather Station (Wx.tempe.gov), where wind is measured with an anemometer at 10 m above ground and the average wind velocity is recorded every ten minutes. The Weibull distribution of wind velocity surrounding Tempe area can be calculated as below:

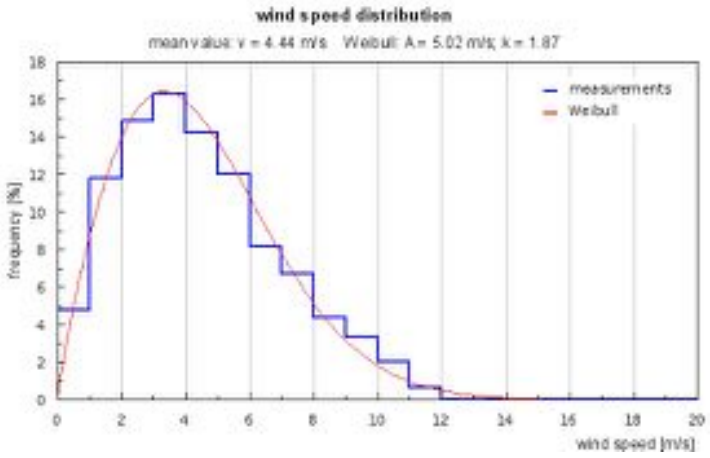

Figure 2.2: Weibull distribution estimation for Tempe wind velocity based on statistics from Town Lake weather station

Where the average wind velocity at observation center is calculated as approximately 4.4 m/s at 10 m altitude, with shape factor k equals 1.87. The log-scale profile is then codded in User Defined Function in Ansys based on the previous discussions from Chapter. 2. The velocity at inlet used in the simulations is shown in Fig 2.3.

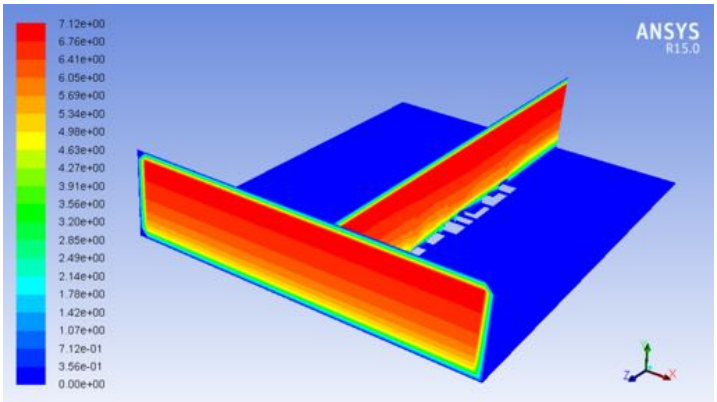

Figure 2.3: Logarithmic velocity profile at inlet boundary of the simulation domain

Logarithmic profile on vertical axis is programmed in Ansys UDF and input as inlet boundary conditions for the simulation.

For most of the small wind turbines, the cut-in speed are between 3~4 m/s, which means the roof turbines are highly likely to be inoperable or cannot produce sufficient amount of energy due to low wind speed in Tempe area. To gain higher efficiency of rooftop wind turbines, the acceleration of wind speed on buildings should be seriously considered and put into good use.

2.3 Wind acceleration over buildings

Separation happens where the flow separates or leaving the surface of the building forming recirculation area behind it, where the flow in that area is mostly characterized by flowing in a reverse direction of the main flow (Abohela 2012). The point where flow separates is called separation point. The word ‘separation’ is used to distinguish smooth flow near surface of the building and the flow that forms bubble on top of the building. Normally separation happens with sharp edged buildings, high energy is gained at separation point thanks to high levels of turbulence, which means if a wind turbine is installed in the high turbulence zone where flows separate, it could generate significant amount of electricity without the need of high-rise mounting poles.

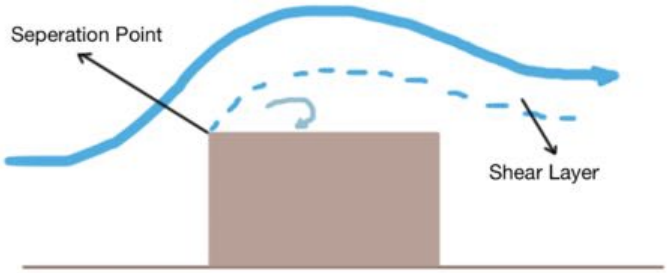

Figure 2.4: Locations of separation point and separation bubble on top of a cube under influence of turbulent flow

Because of the pressure difference at building surface and top of the separation bubble, the wind speed increases comparing to the wind speed at the same altitude without buildings in place. It was found that this accelerating effect is tightly related to the building height while independent of building length (Yeo *et al.* 2011). It was concluded that building height is a key factor influencing the accelerating phenomenon around a single building: the higher the building is, the more the accelerating effect there will be. As the place of separation bubble matters a lot when deciding wind turbine installation locations. Multiple simulations will be performed in this thesis to predict the approximate acceleration zone structures.

2.4 Numerical Simulation Models

There are many previous researches that gives the particle guidelines for CFD modeling of Atmospheric Boundary Layer simulations based on their experience (Castro and Graham 1999; Hu 2003; Franke *et al*. 2007; Abohela 2012). These guidelines address all the steps of a CFD modeling focusing on five main categories; defining the physical model, the geometry of studied problem, the computational domain dimensions, the computational domain boundary conditions and the computational mesh.

There are several physical models to predict airflow around buildings, including DNS, LES and RNS. For the Direct Numerical Simulation (DNS), Navier-Stokes equations are solved directly without approximation, as this kind of simulation requires huge number of cells and time

steps, DNS simulation is currently inapplicable for simulations under Reynolds number of engineering interest.

According to Franke *et al.* (2007), The choice of the basic equations has the largest impact on the modelling errors and uncertainties. One priority problem it should determine is whether the application requires a steady treatment or not. As the atmospheric boundary layer flow is turbulent, an unsteady treatment as in Fig 2.5 is required in principle (Crasto 2007).

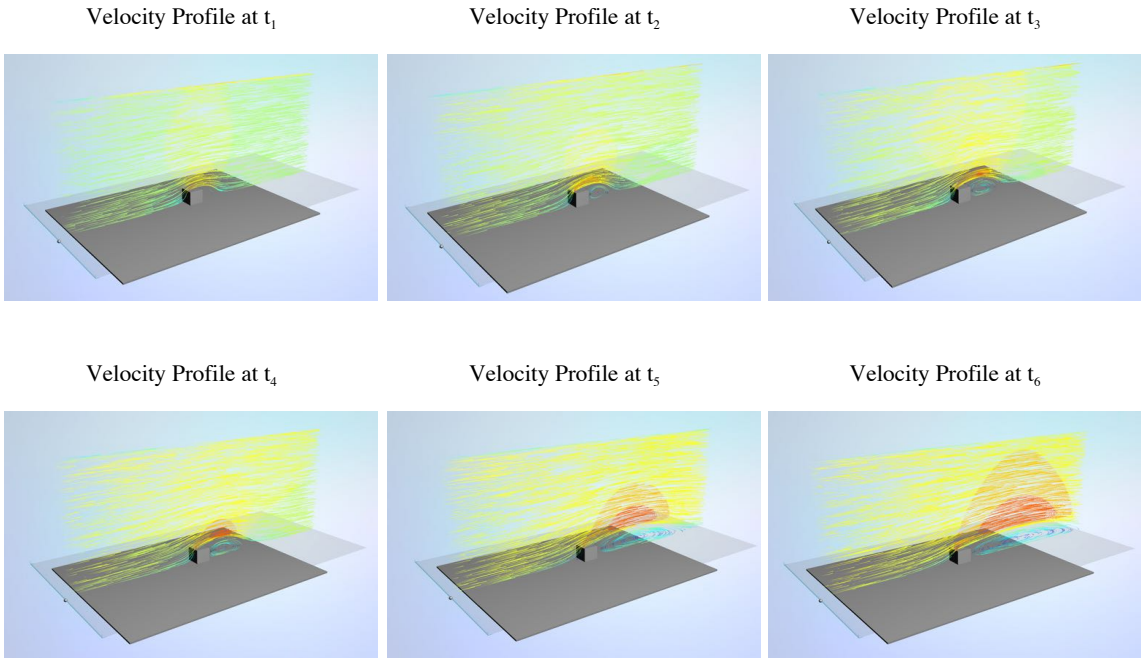

Figure 2.5: Unsteady flow simulation of 10 m/s wind blowing cross 10 m^3 cube structure, vector contours are from Autodesk Flow Design

By time averaging (ex. RANS) or space filtering (ex. LES) turbulence equations, these equations are simplified to be numerically solvable. Additional unknowns turbulence stresses or sub-grid stresses are introduced and a set of equations are constructed based on simplified assumptions.

One of the most commonly adopted methods for solving turbulence structures is the time-averaged approach, which mostly referred to Reynolds Averaged Navier-Stokes (RANS) method.

On the other hand, the space-filtered models directly simulate large eddies and models the small eddies with some assumptions. However, it still needs to resolve the flow fields at stepwise which requires high computational power but less than DNS because it only solve eddies larger than length scale and approximated smaller eddies which do not affect the mean flow. LES is considered one of the most ideal models for CFD simulation of ABLs, as it shows high accuracy in predicting main turbulence properties. One problem about LES approach is that the simulation is time consuming and needs high performance computers for complicated geometry as urban models.

Two turbulence models of RANS approached are commonly adopted for environmental flow simulations, $k-\varepsilon$ and $k-\omega$ models. $k-\omega$ model is used more for prediction of low-Reynolds number flows, near wall flow for example. Moreover, $k-\omega$ simulation method requires high-resolution meshes, so only $k-\varepsilon$ model is put into use for simulations in this thesis.

Standard $k-\varepsilon$ function performs poorly in predicting flow separations under the action of adverse pressure and curved boundary layers flow. For a better description of turbulence models, realizable $k-\varepsilon$ turbulence model is chosen.

Realizable $k-\varepsilon$ model was developed based on modification of the dissipation rate (Ɛ) equation to satisfy certain mathematical constraints on the normal stresses consistent with the physics of turbulent flows. As for the turbulent kinetic energy (k) equation, it is the same as that in the standard k-e turbulence model (Varghese, Frankel and Fischer 2008). One thing to mention is that the production term in the dissipation rate (Ɛ) equation does not involve the calculation of k parameter, which gives a better representation of the spectral energy transfer of turbulent flows (Lei *et al*. 2006). Moreover, realizable $k-\varepsilon$ fixes the false production of turbulent kinetic energy around the stagnation point, which is one of the greatest drawbacks of standard $k-\varepsilon$. In conclusion, realizable $k-\varepsilon$ will give better results for boundary layers under strong pressure gradients and flow separation at stationary point compared to other RANS models. (Mertens 2006)

2.5 Influence from installation of Wind turbines

As the project focuses mainly on predicting wind acceleration phenomenon on building tops and the feasibility of putting a wind turbine in the acceleration zone to gain higher energy ratio, it is very important to make sure that the acceleration zone over building tops won't affected by installment of wind turbines.

CAD models containing a 10x10 m box with and without a 1 m wind turbine on top are tested in Ansys Fluent under logarithmic ABL profile. The wind turbine remains still and only act as an obstacle to examine geometry affects on accelerations. Results are then compared to identify the effect from wind turbine installation.

The velocity contour in the center plane is as in Fig 2.6, as can be observed in the figures, the left shows a cube without wind turbine on top while right has a wind turbine mounted on the upper right corner.

Velocity Profile without Wind turbine on top

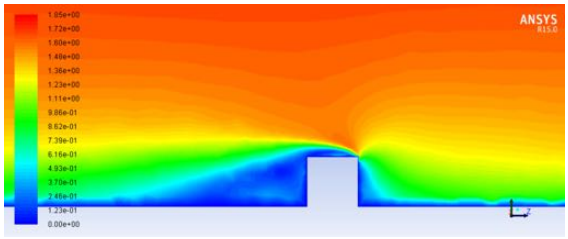

Velocity Profile with Wind turbine on top

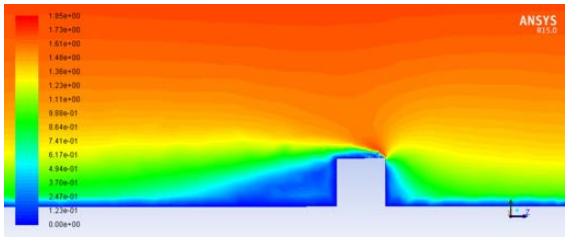

Figure 2.6: Velocity contour of 10 m/s wind blowing cross 10 m^3 cube structure with and without wind turbine on top

The contours show no significant structure change in the vortex shape and locations, separation bubbles on cube top and vortex behind the cube all look the same. Quantitatively, the maximum velocity also remains unchanged (7.4 m/s) in both cases. Further zoom in of the contours are shown in Fig 2.7, several lines of interest are insert into the contours, velocity magnitude data is taken along these lines.

Velocity profile without wind turbine on top (zoom-in)

Velocity profile with wind turbine on top (zoom-in)

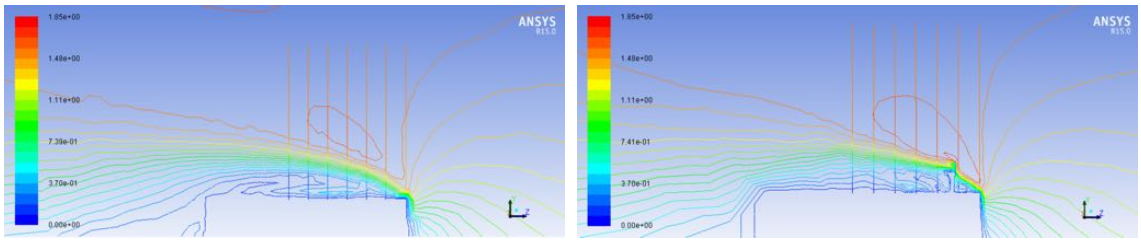

Figure 2.7: Velocity contour of 10 m/s wind blowing cross 10 m^3 cube structure with and without wind turbine on top (zoom-in)

As mentioned, velocity magnitude along vertical lines are recorded and plotted. The vertical lines of interest are picked up 0-6 m offset from corner of the box. Velocity at the same height at inlet boundary is also plotted in the graph, dots to the right of the inlet boundary can be considered as accelerated.

Velocity magnitude without wind turbine on top

Velocity magnitude with wind turbine on top

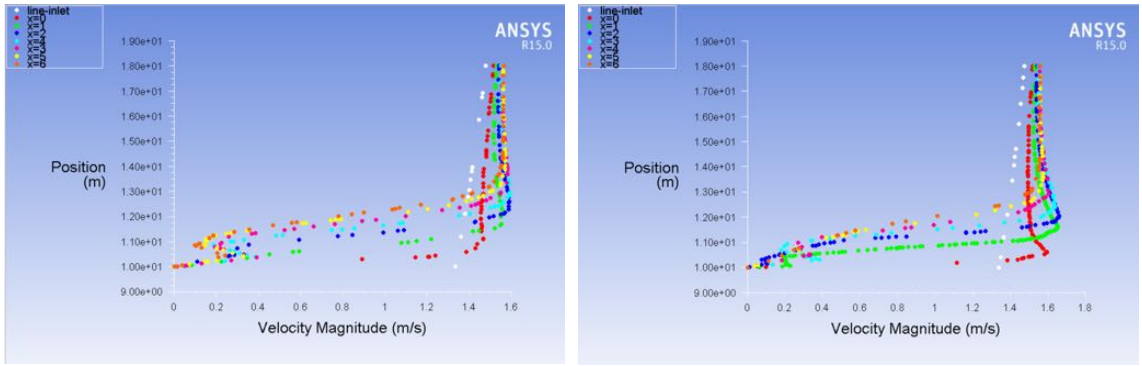

Figure 2.8: Position-velocity magnitude plots of with and without wind turbine on cube top, white dots represent inlet velocity.

It can be concluded from figure 2.8 that noticeable velocity difference happens at zero offset from corner, where the wind accelerated greatly near building surface due to second acceleration caused by wind turbine geometry. However, velocity acceleration behavior along other lines is not affected much by the geometry change. Which leads to the conclusion that simulation results are still acceptable even without small wind turbine on building tops.

Chapter 3

WIND ACCELERATION OVER ROOFTOPS IN ASU CAMPUS

3.1 Introduction

As discussed in the previous chapter, RANS approach and logarithmic inlet boundary layer would be used for simulations; further parameter settings during the simulation will be discussed in this chapter. A flow chart showing structure of this chapter is as below:

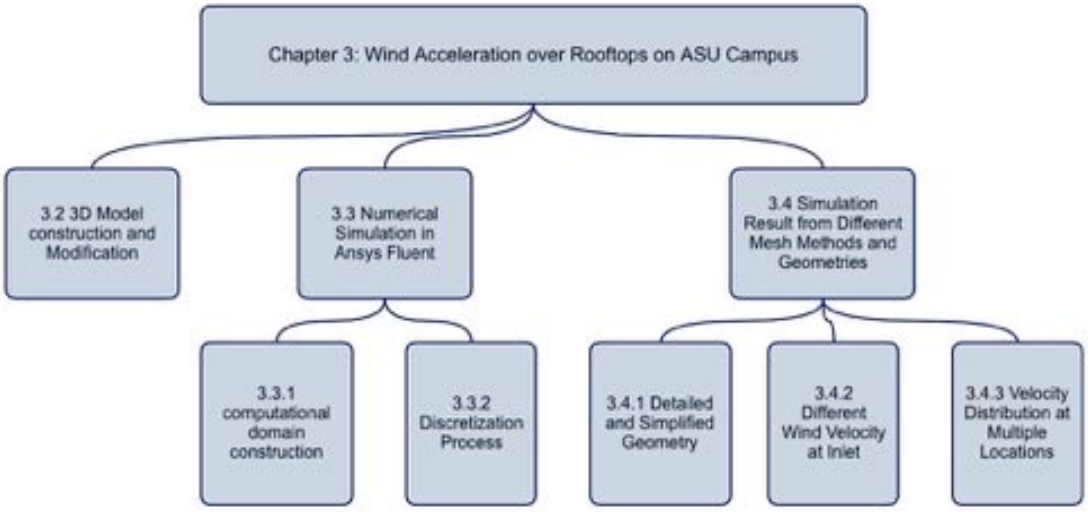

Figure 3.1: Chapter structure overview

3.2 3D Model construction and Modification

Several less-ideally mounting site of wind turbines are presented in chapter one, one of the cases them is located on ASU campus. In this case, six parapet wind turbines were mounted on the roof of Global Institute of Sustainability building, Even though Wind speeds of 27 mph or higher allow the turbines to generate maximum power, these turbines can also produce electricity with winds down to five miles per hour according to the official website (sustainability.asu.edu).

To examine the hypotheses that ASU campus are not suitable for small wind turbine

installations. A part of ASU campus with multiple high-rise buildings was selected for the simulation, as marked in orange region in Fig. 3.2, the selected region contains the top four highest buildings in Tempe campus, as marked in the picture.

Figure 3.2: Satellite map of a corner of ASU campus. Areas within the orange box contains multiple highest buildings on campus are selected as the simulation domain.

GIS datasets from ASU GIS Data Repository and building details from Google map were used as a reference for the model construction, with that a relatively detailed model was obtained as in Fig. 3.3.

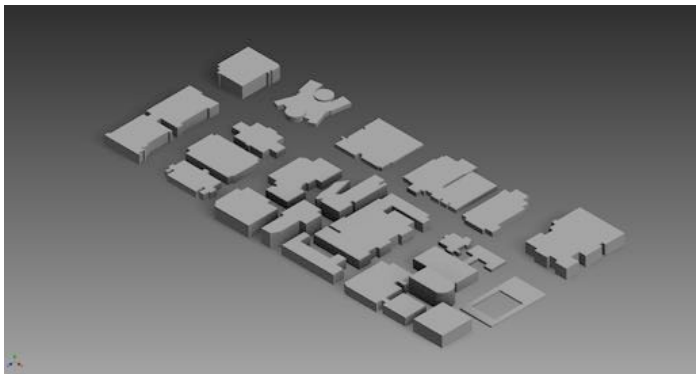

Figure 3.2: Relatively detailed geometry of a corner of ASU campus. Building on the upper left corner is ISTB4, building on the upper left corner is the Social Science building

Normally the overall geometry of buildings has a great impact on wind flow patterns. Details including gaps and roof shapes or even balconies can affect the final simulation result. The nearer the individual building is to the building of interest, the more detailed it should be to

fulfill the accuracy requirement. Despite the fact that accuracy of the simulation results in Ansys Fluent are well related to 3D geometry resolutions, overly detailed building model can lead to low mesh quality and huge amount of cell numbers, which not only costs incredibly long calculation hours but also results in low quality of the meshes. In this chapter, the tallest building on upper left corner of the geometry (ISTB4) is chosen as the building of interest and influence of geometry detail is examined in Autodesk Flow Design. To reduce the mesh and simulation time cost, the model above is then simplified in Autodesk Inventor as shown below:

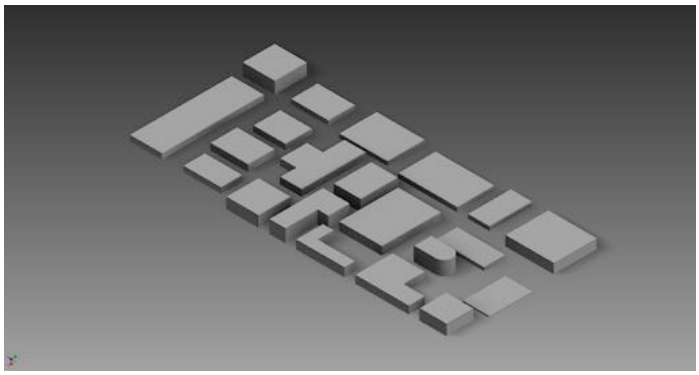

Figure 3.3: Simplified geometry of a corner of ASU campus. With block on the upper left corner representing ISTB4, block on the upper left corner is the Social Science building

To make sure the elimination of building details won't ruins simulation, models before and after simplification are input into Autodesk Flow Design to run a quick test of wind distribution, though the result is within 75-80% accuracy in regards to drag coefficient, it manages to tell the difference between two simulation results and whether error caused by simplifications of geometry is acceptable or not. Further discussion on the simplification of geometry will be included in section 3.2.

On the other hand, another problem while dealing with urban model in Ansys lies in the scale down of geometry, as most full-scale geometry cannot fit in Ansys Design modeler, ¼ size geometry is adopted in this project, to make sure the size down won't affect simulation results too much, full-size simplified geometry is compared with a ¼ size detailed geometry as below:

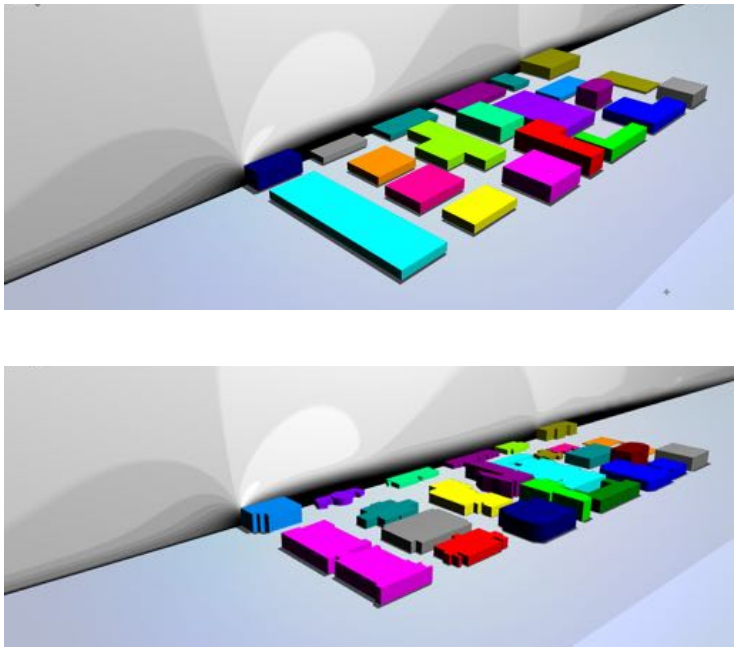

Figure 3.4: ¼ scales detailed (top) and Simplified (bottom) geometry of a corner of ASU campus. The simulation is performed in Autodesk Flow design with 10 m/s velocity at inlet and zero pressure at outlet

As result doesn't see an obvious difference in the wind velocity and distribution, it can be concluded from the figures above that the simplified geometry will lead to some differences in results but the differences is within acceptable range at this level of simulation.

Once making sure the less detailed model works equally well in this simulation, the simplified model can be inputted into Ansys Fluent for further analysis.

3.3 Numerical Simulation in Ansys Fluent

3.3.1 computational domain construction

The size of the entire computational domain in vertical, lateral and flow direction depends on the geometry of interest and on the boundary conditions used. For single buildings the guidelines of Hall (1997) can be applied. The inlet, the lateral and the top boundary should be 5H away from the building, where H is the building height. For buildings with an extension in lateral direction much larger than the height, the blockage ratio should be below 3% (Tominaga *et al*.).

Moreover, to prevent an artificial acceleration and unexpected velocity decrease near computational domain rooftop. Vertical distance of the computational domain should be at least $5H_{max}$ away from tallest building.

In some previous simulations, cylindrical domain was also used to predict wind profile when considering wind coming from different directions. In this case, the cylinder height should also follow the $5H_{max}$ rule.

As geometry is scale down to ¼ of the original size in this project, simulation domain is built based on the scaled size of the tested domain as in Fig. ., the tallest buildings are highlighted with color:

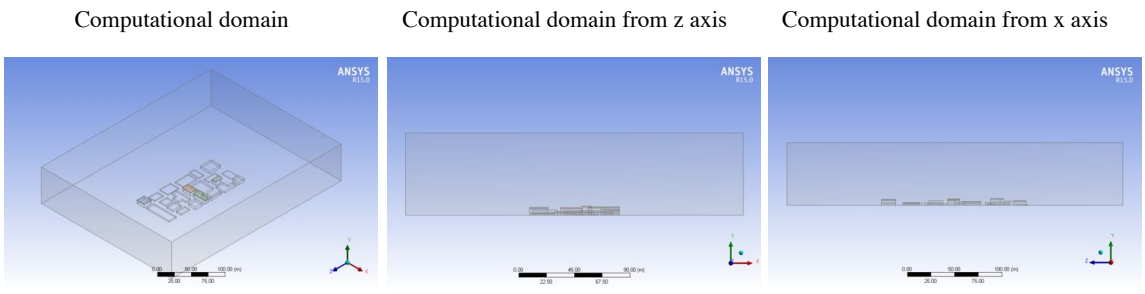

Figure 3.5: Computational domain in Ansys design modeler looking from different directions, the domain is constructed based on the instructions above.

The final computational domain is 272.5m in X direction, 335m in Y direction and 66.5m in Z direction, which is approximately 12 times the height of the tallest building.

3.3.2 Discretization Process

CFD solution accuracy is highly depended on number of cells. Basically, the greater the number of cells is, the higher accuracy will be. However, it should be considered that with enlargement of cell numbers, the computation cost also increases and longer computational hours is needed. Therefore, the optimal approach is to use non- uniform meshes. Which means use finer mesh where there are large variation from point to point and coarser mesh in regions with more steady transits. For the wind simulation in this case, the purpose of the

whole project is to get the velocity on top of high-rise buildings, which means lower resolution for other parts of the computational domain is allowed. For most cases with simpler geometry containing one or several square buildings, structured hexahedral grid is computed with refined grid near the model.

For complicated geometry as ASU campus model in this project, a combination of hexahedral and tetrahedron mesh cells could also be considered to better describe the geometry and faster convergence in less iteration.

However, as we are not dealing with high-energy dynamic events that involve impact or shock loads, which requires explicit analysis, 4-noded tetrahedral is acceptable and widely used for implicit cases like this for the seek of larger stability time steps.

In this project, various discretization methods in Ansys are simulated to find the best way to mesh an urban ABL domain as explained in the following paragraphs.

The quality of the mesh plays a significant role in the accuracy and stability of the numerical computation. Which makes mesh quality checking before running the simulations essential. There are a couple of indicators in Ansys Fluent that can be used to tell whether the mesh is good or not, one important criteria among them is the orthogonal quality. The following parameters are calculated for each face to get the orthogonal quality (VirginiaTech ARC):

The normalized dot product of the area vector of a face ($\overrightarrow{A_i}$) and a vector from the centroid of the cell to the centroid of that face ($\overrightarrow{f_i}$):

$$\frac{\overrightarrow{A_i} \cdot \overrightarrow{f_i}}{\left|\overrightarrow{A_i}\right| \cdot \left|\overrightarrow{f_i}\right|}$$

The normalized dot product of the area vector of a face ($\overrightarrow{A_i}$) and a vector from the centroid of the cell to the centroid of the adjacent cell that shares that face ($\overrightarrow{c_i}$):

$$\frac{\overrightarrow{A_i} \cdot \overrightarrow{c_i}}{\left|\overrightarrow{A_i}\right| \cdot \left|\overrightarrow{c_i}\right|}$$

The minimum value from two equations above for all of the faces is then defined as the orthogonal quality for the cell. Therefore, the worst cells will have an orthogonal quality closer to 0 and the best cells will have an orthogonal quality closer to 1.

Another important indicator of the mesh quality is the aspect ratio. The aspect ratio is a measure of the stretching of a cell. It is computed as the ratio of the maximum value to the minimum value of any of the following distances: the normal distances between the cell centroid and face centroids, and the distances between the cell centroid and nodes (Bern, Eppstein and Gilbert 1994). The aspect ratio of an ideal tetrahedral element is 1.0. This is a ratio of the longest edge to the shortest normal dropped from a vertex to the opposite face, normalized with respect to the shortest normal dropped from a vertex to the opposite face of a perfect tetrahedral element. A general rule of thumb is to not have more than 10% of the elements with an aspect ratio higher than 10. Extremely large values >> 40 should be closely examined to determine where they exist and whether the stress results in those areas are of interest or not.

One of the less time-consuming ways is to mesh with only by tetrahedron cells, this kind of mesh is widely used in complicated cases to better describe the detail of the buildings, an automatically generated tetrahedron mesh at fine grid with minimum edge length of 0.5m is obtained from Ansys Fluent as in Fig 3.6.

Mesh elements in horizontal plane

Mesh elements in vertical plane

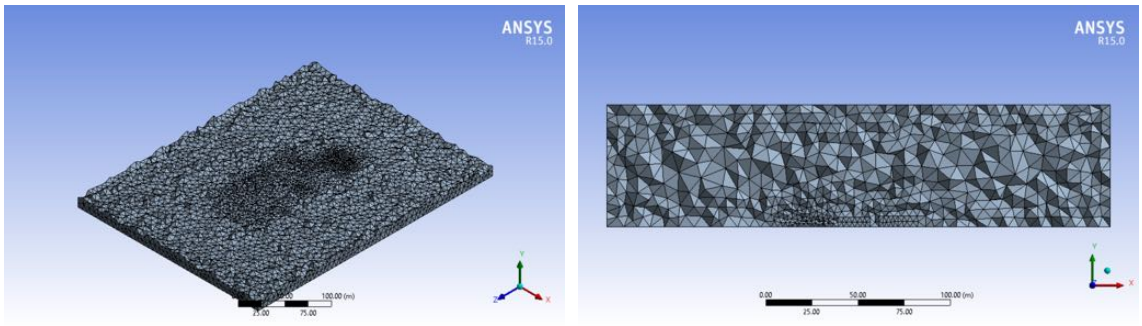

Figure 3.6: Mesh elements on horizontal (left) and vertical (left) slice planes. The domain is meshed with tetrahedron cells only

Based on the statistics from Ansys Fluent, the orthogonal quality of the mesh is 2.41135e-01, with maximum aspect ratio of 1.93485e-01. Which indicates the mesh is useable but not in very good quality. Further simulations in Ansys Fluent indicate that huge amount of turbulence structure details are almost totally wiped out due to low resolution and poor mesh quality, the maximum velocity is also slightly off. In all, it is safe to say that using automatically generated mesh is unacceptable in simulations like this. Velocity contours from this meshing method is shown in Fig. .

Velocity magnitude contour

Velocity magnitude contour (zoom-in)

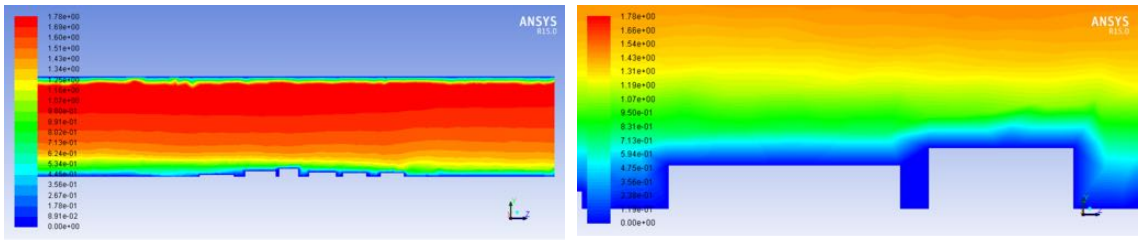

Figure 3.7: Velocity magnitude contour of the whole slice plane (left) and zoom-in result (right). The zoom-in result shows no acceleration due to low mesh quality

Another recommended way is to use a combination of hexahedral and tetrahedron for meshing process, this kind of mesh usually results in a discontinuity at lower meshing resolutions as in Fig 3.8.

Mesh elements in horizontal plane

Mesh elements in vertical plane

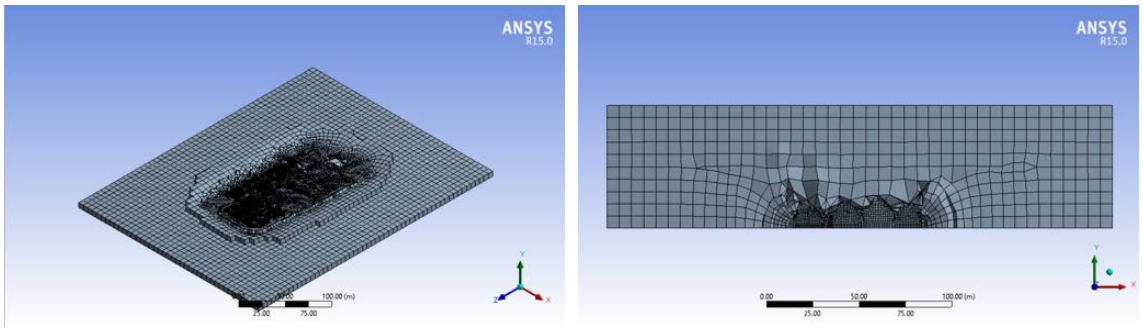

Figure 3.8: Mesh elements on horizontal (left) and vertical (left) slice planes. The domain is meshed with combination of hexahedral and tetrahedron cells together

The minimum orthogonal quality goes to zero and aspect ratio to 1.42034e+02, which means the case can't be process in Ansys Fluent before mesh is adapted. After adaption, the nodes number is recorded as 213500 and elements number of 268871, this number difference is due to tetrahedron cells been mixed with hexahedrons. Velocity magnitude contour is obtained after adaptation of the cells, as in the figures below, the result not only sees inaccuracy of the profile but also rapid changes in cell volume, which may lead to large truncation errors. However, the automatically generated tetrahedron meshes near building surface are relatively smoother.

Velocity magnitude contour

Velocity magnitude contour (zoom-in)

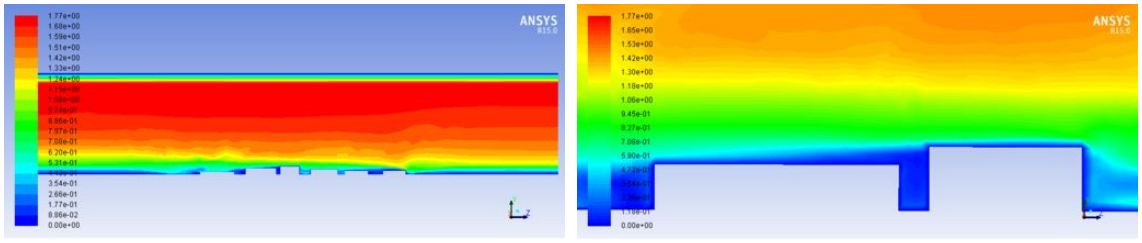

Figure 3.9: Velocity magnitude contour of the whole slice plane (left) and zoom-in result (right). The zoom-in result shows a relatively high resolution surrounding the buildings, but discontinuity occurs at the border of different meshing elements

One recommended approach is to generate hexahedron mesh is in Ansys ICEM, which gives relatively high quality meshes. Most researchers dealing with Atmospheric Boundary Layer simulation these days use pure hexahedron mesh for better convergence. In Ansys, ICEM is

applied for more accurate meshing near ground. ICEM makes it possible to divide the whole domain into multiple blocks and mesh them separately based on requirements. In this case, a structured hexahedral grid is employed in the vicinity of the buildings (facades and roof) for higher accuracy. A structured grid of larger size will also be used in the upstream, downstream and lateral regions relatively far away from the buildings (Weerasuriya 2014).

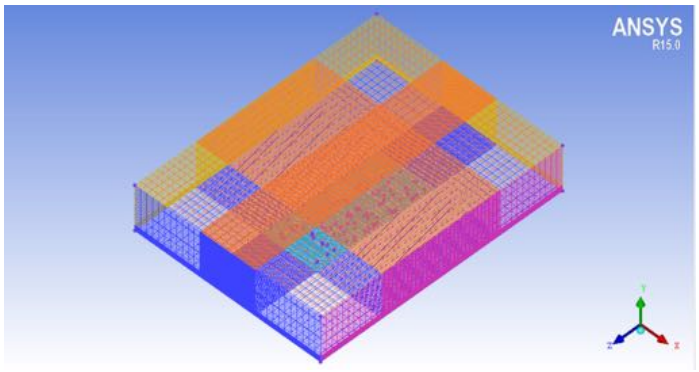

Figure 3.10: ICEM mesh result looking from corner

This kind of mesh can best fit in with geometry and all the near-wall regions are perpendicular to the building walls. However, pure Hexahedral mesh does not body fit building boundaries too well, as can be seen in Fig. . The only way to fix this problem is by using sufficient fine mesh resolution to represent building details. In other words, great number of elements is required to accurately describe complex geometry like this with hexahedrons. Which is inoperable on computers at this level.

ICEM mesh in vertical plane

ICEM mesh in vertical plane (zoom-in)

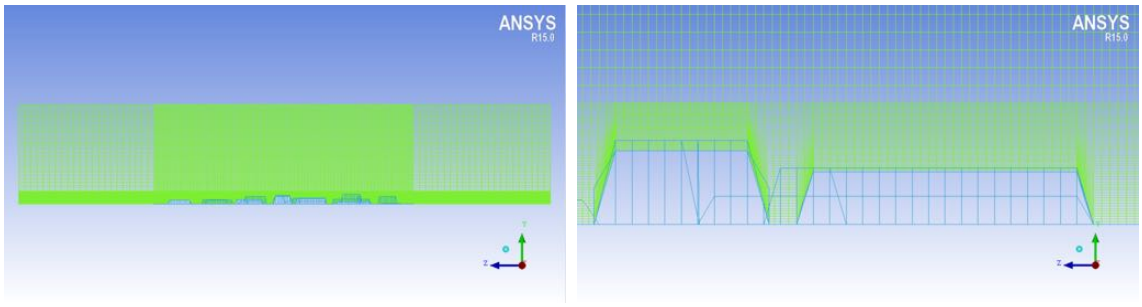

Figure 3.11: ICEM mesh result in vertical plane looking from x direction and zoom-in result

showing mesh cells at geometry boundary

To obtain a better resolution in the region of interest while maintaining a relatively lower computational cost, tetrahedral elements method with building top region refined is applied. Domain of influence is set on few top highest buildings in Ansys DesignModeler as in Fig 3.12.

Mesh elements in horizontal plane

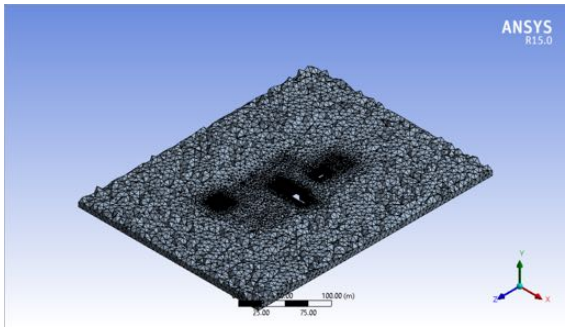

Mesh elements in vertical plane

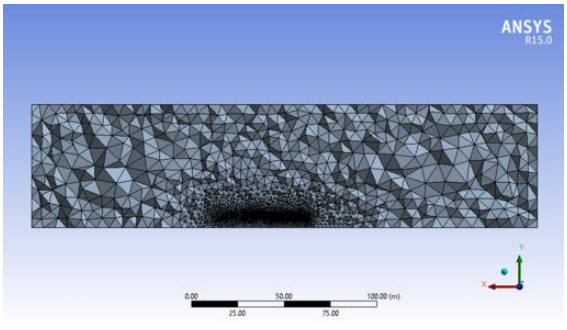

Figure 3.12: Mesh elements on horizontal (left) and vertical (left) slice planes. The domain is meshed with tetrahedron cells only and further refined at top of buildings of interest

According to mesh quality checks from Ansys Fluent, the orthogonal quality of the mesh is 3.59090e-01, with maximum aspect ratio of 1.40622e-01. Which is significantly better than the indexes before mesh refinement. The node number and elements number are 179404 and 1002246 separately. Simulation result at the same slice plane as previous cases is shown below:

Velocity magnitude contour

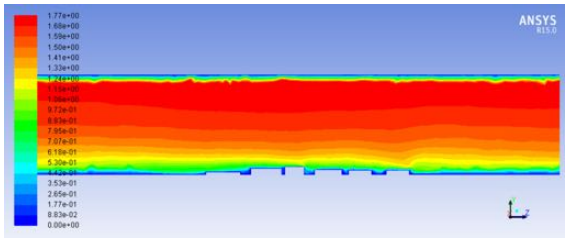

Velocity magnitude contour (zoom-in)

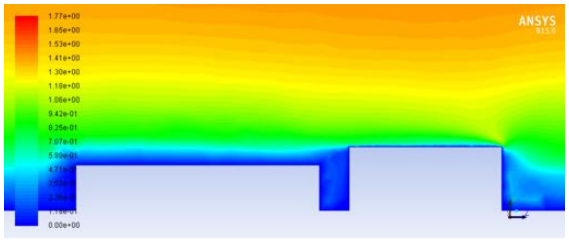

Figure 3.13: Velocity magnitude contour of the whole slice plane (left) and zoom-in result (right). The zoom-in result shows a significant acceleration zone on building top, which indicates a higher resolution than the previous mesh methods

By comparing the multiple zoom-in contours of velocity profile on building tops, one can easily reach the conclusion that the tetrahedron method with mesh refinement endures the

highest resolution among all cases, as it is the only method showing turbulence structural details and vortexes behind buildings, mean well the velocity contour is smoother than other settings as well.

Further analysis of mesh quality is performed based on dimensionless wall distance y plus parameter.

$$y^+ = \frac{U_\tau y}{\upsilon}$$

Where $U_\tau$stands for the friction velocity at nearest wall, y is the distance to the nearest wall and υ is the local kinematic viscosity of the fluid.

Further more, y+ can be used to quantify the mesh resolution in the near-wall regions. The near-wall model approach requires the use of meshes with a high mesh density in the near-wall regions. The $k-\mathcal{E}$ models are not capable of resolving the near wall flow and therefore 30 < y+ <300 should be reached. Other two-equation models, such as the $k-\mathcal{E}$ model are capable of resolving the near-wall flow without wall-functions at sufficiently high mesh resolutions (y+ < 5) (Menter 1994).

The y plus value of the ground is plotted in Ansys Fluent as below, y plus lies between 30-4500, which significantly exceeds the recommended value.

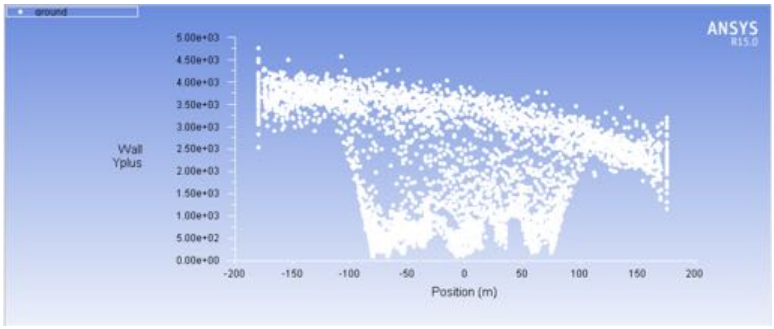

Figure 3.14: y plus value near the ground surface distribution from Ansys Fluent, the results exceeds the recommended value of 1000

This is a known issue in ABL simulations as this one, and some discussions are made upon this issue. Standard wall functions are typically also used in CFD simulations of atmospheric boundary layer wind flow when y+ is well above the upper limit of 500–1000 without reduced performance for the velocity field. This is also demonstrated in previous validated CFD studies in which y+ values with the same order of magnitude were used. The most important reason for using these high y+ values is that the recommended range of y+ values (30–500) would yield unnecessarily small near-wall cells (van Hooff, Blocken and van Harten 2011).

One possible way to solve this problem is by explicit modeling the roughness elements, which gives better results based on some previous works (Blocken *et al*.). As the relation $y_p > K_s$ is obeyed. Because of modeling the roughness elements there is no need to define high scale roughness parameters (i.e 0.5-3 m) in rough wall functions, and there for lower scale roughness parameters (i.e 0.01-0.1) are defined for the functions and this results in a lower y_p and therefore better y+ values. In this case additional drawback are the increased number of cells and the subsequent increase in required computing power and CPU time.

3.4 Simulation Result from Different Mesh Methods and Geometries

3.4.1 Detailed and Simplified Geometry

To further discuss the influence of building geometry simplification, two sets of ASU building models from section 3.2 are tested under same simulation settings in Ansys Fluent under medium wind velocity profile, the results show some differences but are within acceptable range.

Velocity contour – detailed geometry

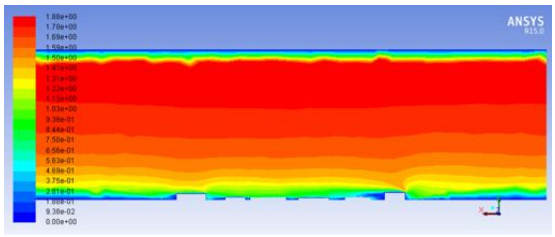

Velocity contour – detailed velocity (zoom in)

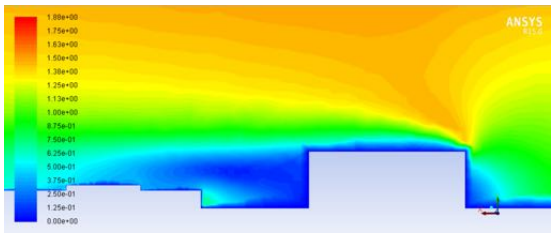

Velocity contour – simplified velocity

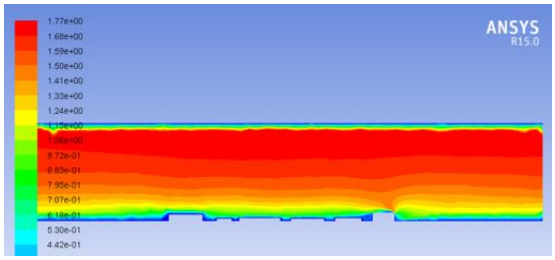

Velocity contour – simplified velocity

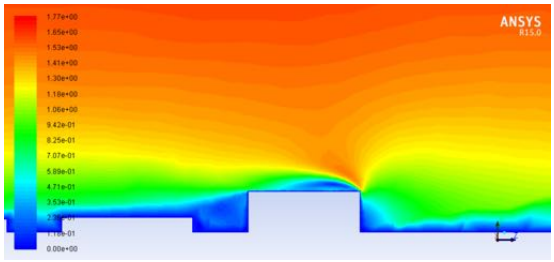

Figure 3.15: Detailed geometry velocity magnitude contour of the whole slice plane (left) and zoom-in result (right). The computational time is quite long in this case

It can be observed from the contours that the velocity distributions over ISTB4 are similar to each other, but the simplified geometry seems to show a better resolution of vortexes, this is due to mesh refinement performed only on simple geometry cases as below, as refinement of a complicated geometry is much harder and simulation is significant time consuming (about ten times computational cost of the simplified cases), no further refinement is performed on detailed geometry in this case.

Mesh elements – detailed geometry

Mesh elements – detailed velocity (zoom in)

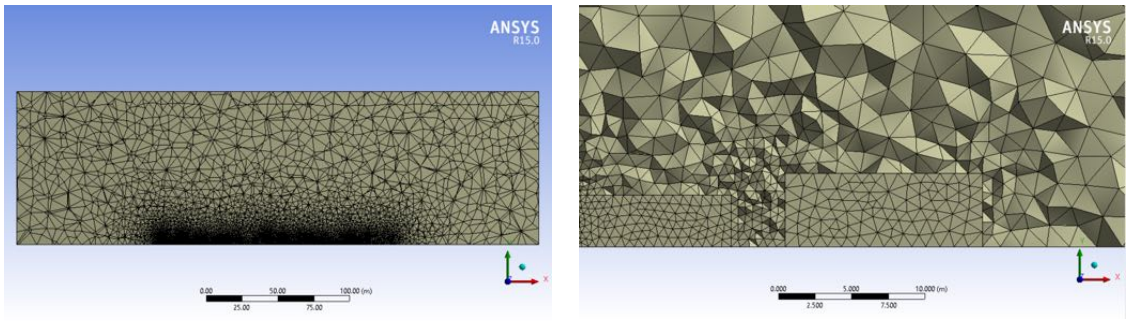

Mesh elements – simplified velocity

Mesh elements – simplified velocity

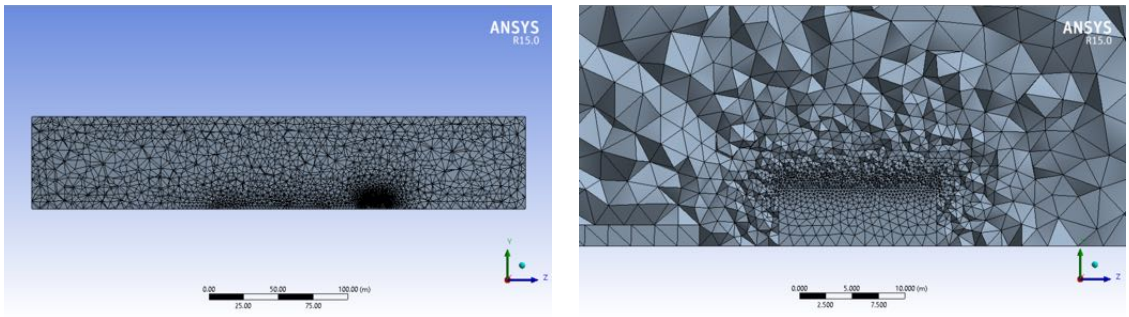

Figure 3.16: Mesh comparison of detailed geometry (top) and simplified geometry (bottom). The detailed geometry are not refined on building tops as did for the simplified geometry case

As shown in the mesh figures above, the mesh resolution on ISTB4 has been refined using mesh sizing tool in Ansys for a higher resolution and more data points, so when zooming in the mesh elements picture, simplified geometry case has much more cells comparing to the detailed one.

To assess how much the wind has accelerated on building tops, we adopted a criterion, accelerate ratio R_a by comparing velocity on building tops with velocity at inlet at the same altitude, R_a is defined as below:

$$R_a = \frac{V_T}{V_B}$$

Where V_T and V_B stand for wind velocity on building tops and at inlet respectively.

As most of the roof turbines will be installed no higher than 8 meters above building tops, and most significant acceleration zone is close to building edges facing the inlet. V_T along the vertical lines as below is documented and compared with V_B from inlet at same altitude, each line is 4m from each other.

Velocity contour on building top – detailed geometry

Velocity contour on building top – simplified geometry

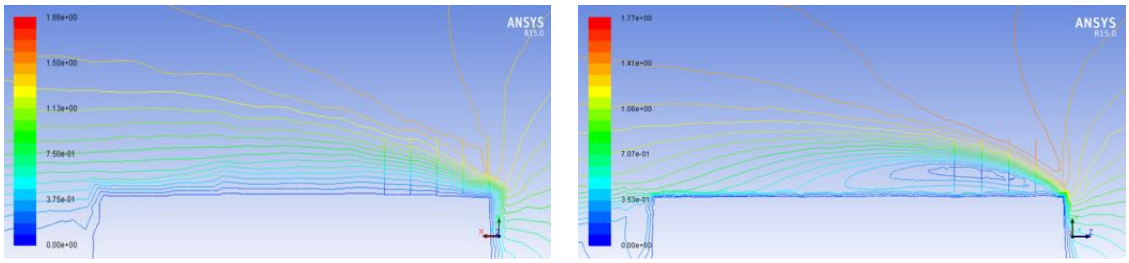

Figure 3.17: Velocity contour of detailed geometry (left) and simplified geometry (right). The line-of-interest in inserted at the same location in both cases

The calculation result of R_a is plotted as below. As shown in the graph, the trend of the plots is similar, for in both cases the greatest acceleration happens at building edges (x = 0 m) at lower altitude, and acceleration ratio goes down gradually after reaching the maximum point. As mentioned previously, the mesh for detailed geometry has lower resolution on ISTB4 roof, which results in the 'disappearance' of vortex on building tops.

Velocity magnitude plots – detailed geometry

Velocity magnitude plots – simplified geometry

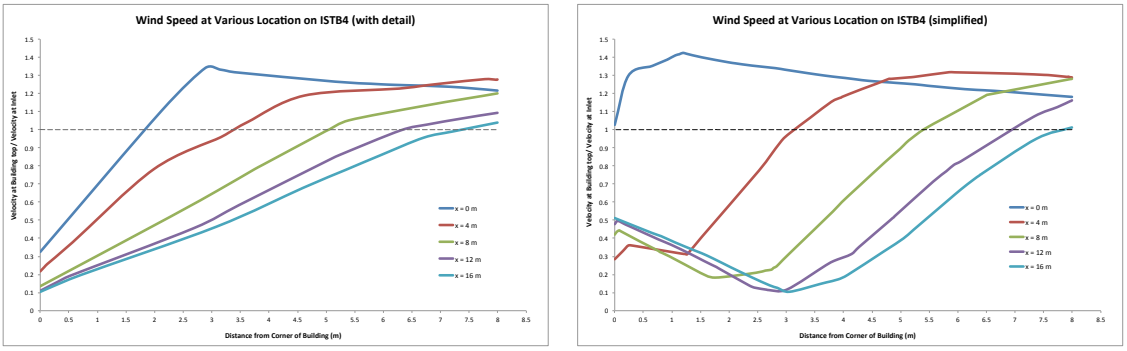

Figure 3.18: Acceleration ratio plots of detailed geometry (left) and simplified geometry (right). Both cases see a noticeable acceleration at top of building, although due to low resolution near building surface in detailed geometry case, velocity changes are not shown and plots are shown as straight lines

Another thing to notice is that while simplifying the geometry in Autodesk Inventor, the bump on the building near ISTB4 to the left is automatically wiped out. Which makes that building shorter than it's truthful model, and results in some differences in the numerical simulation results in return. As the nearer a individual building is to the building of interest (ISTB4 in this project), the more influential it will be to the final simulation results, one should chose carefully how and at where to simplify the geometry. A good way may be wiping out the geometry details further away from the building of interest while keeping the details on buildings closer to it.

3.4.2 Different Wind Velocity at Inlet

As is a matter of common observation, wind velocity is not constant and follows a Weibull distribution, in this section, three representing wind velocities at inlet boundary is chosen for simulations as below, these wind velocity is selected based on the Tempe wind Weibull distribution chart from chapter 2. Three velocities at 10 m above ground are set as baselines: 0.9 m/s, 4.5 m/s and 11.5 m/s.

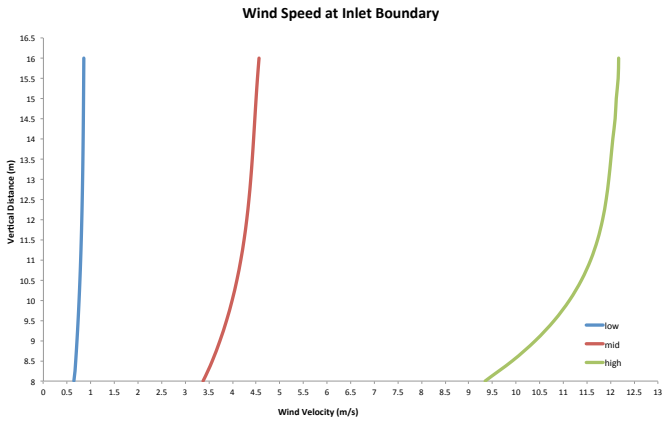

Figure 3.19: Velocity profile chosen for simulation. Low inlet velocity, medium inlet velocity and high inlet velocity.

All the inlet condition is determined based on Tempe wind observation data and is input into Ansys Fluent using UDF manual. Same mesh refinement parameter as in 3.4.1 is adopted as control variable. Simulation result across ISTB4 is listed in Fig 3.20.

Velocity contour – low inlet velocity | Velocity contour – mid inlet velocity | Velocity contour – high inlet velocity

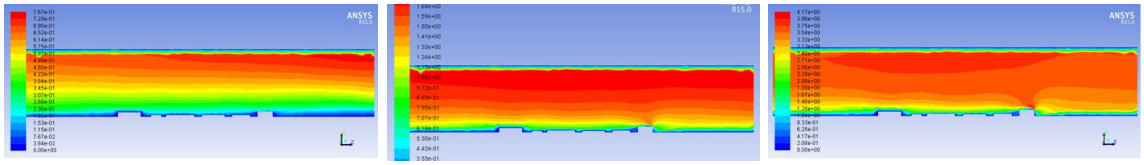

Low inlet velocity (zoom in) | Medium inlet velocity (zoom in) | High inlet velocity (zoom in)

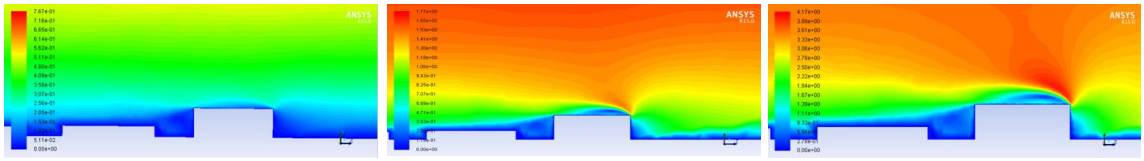

Figure 3.20: Velocity contour at low inlet velocity (left) medium inlet velocity (center) and high inlet velocity (right).

As can be observed from the images above, no significant acceleration can be detected on rooftop of ISTB4 at lower velocity, the Reynolds number is relatively low due to low velocity in the domain, however, at medium and relatively higher inlet velocities, acceleration domain can be easily detected on rooftops of ISTB4. The wind speed data is then documented using the same

method as in 3.4.1.

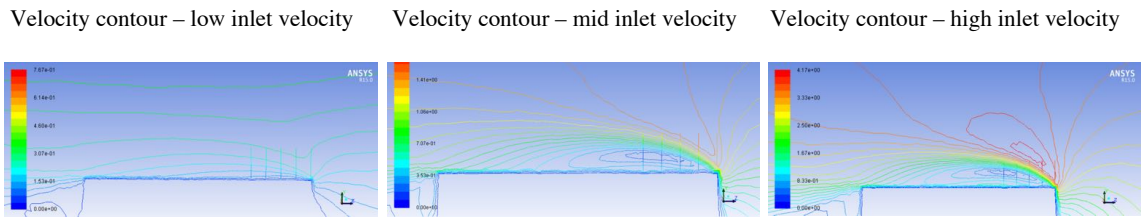

Figure 3.21: Velocity contour at low inlet velocity (left), medium inlet velocity (center) and high inlet velocity (right). The line-of-interest in inserted at the same location in both cases

Results of velocity profile along the lines in each cases are plotted as below, which indicate that the highest velocity happens at 1m distance from edge 6~7m above building top. But that does not indicates that it is the best location to install a wind turbine as wind turbine at higher altitude can lead to maintenance and installment cost problems, ideally roof-turbines should be installed 0.5~1.5m beyond rooftops.

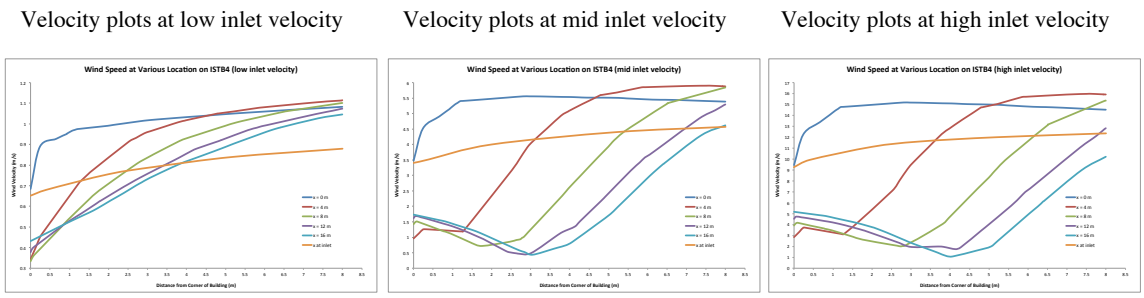

Figure 3.22: Velocity magnitude plots at low inlet velocity (left), medium inlet velocity (center) and high inlet velocity (right).

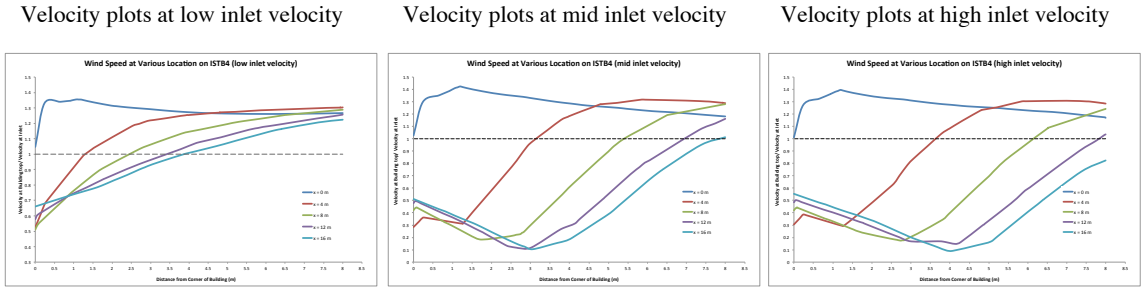

Figure 3.23: Velocity acceleration ratio at low inlet velocity (left), medium inlet velocity (center) and high inlet velocity (right).

For further analysis, accelerate ratio R_a is calculated and plotted as in figure above . As it can be concluded from the plots, the highest velocity acceleration zone in the geometry happens at 1~2m above ground at edge of ISTB4. In other words, wind turbines should be installed at those locations to put wind acceleration energy into full use.

3.4.3 Velocity Distribution at Multiple Locations

As is mentioned earlier, ISTB4 is chosen as the building of interest in this section, however, to fully develop the wind acceleration energy potential at ASU campus area, multiple high-rise buildings are considered including ERC, ISTB1 and LSE. These three buildings and ISTB4 are the top four highest buildings in the considered domain. The buildings are simulated in the medium and high velocity case as both cases see significant velocity acceleration over ISTB4 in previous section. The buildings are highlighted as below:

ASU campus (part) model

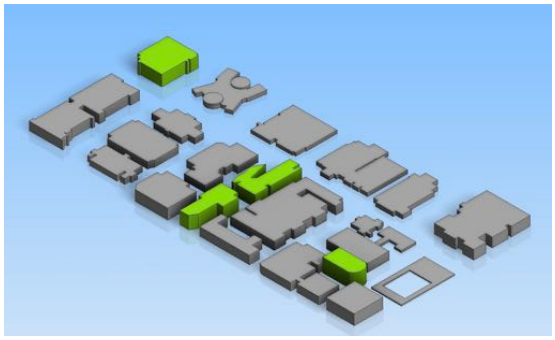

Slice planes setting

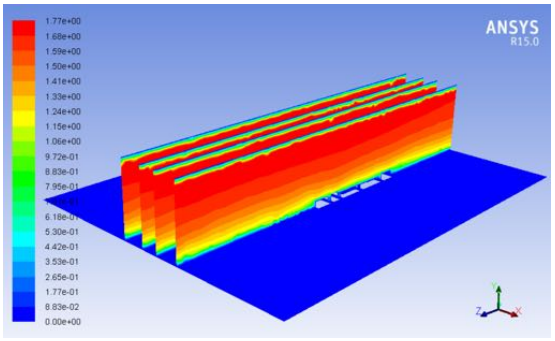

Figure 3.23: Top four tallest buildings in ASU campus are shown in figure at left, slice planes are placed crossed the buildings as in figure in the right.

Four velocity contours can be observe from x direction in the picture above, the results on the sliced planes are shown as below:

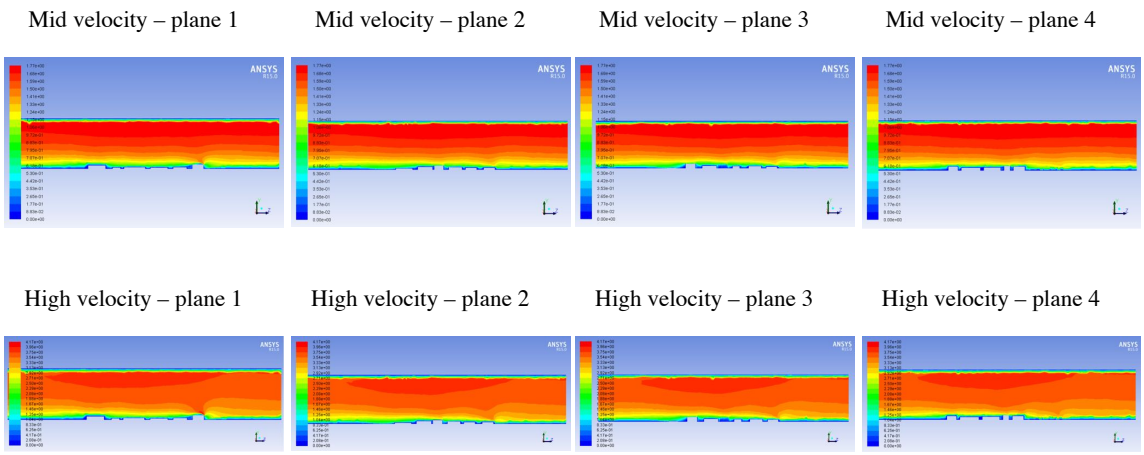

Figure 3.24: Contours on the four sliced are shown in figure at left, slice planes are placed over the top four tallest buildings

The velocity contours of the rest three buildings aren't showing noticeable acceleration zones as on ISTB4 top, moreover, the only obvious accelerations in the contours are on the first buildings facing velocity inlet. This insignificant acceleration on the rest buildings is due to lack of high-rise buildings, no obvious building height difference in other words.

In reality, the chosen ASU geometry is not isolated as in the numerical simulations above, which means that there are other obstacles between ISTB4 and the velocity inlet boundary that contributes to the ground roughness parameter in front of the building, in short, the acceleration of wind on building tops nearest to inlet won't be so noticeable as in simulations. In conclusion, the tested ASU campus domain isn't the best region to install wind turbines die to the lack of high-rise building geometries.

3.5 Conclusion

With respect to small-scale or local wind-energy generation in an urban environment, the following conclusions are drawn from the foregoing discussion:

- For this level of simulation, refined tetrahedron element mesh can give a quick convergence and relatively accurate results.

- Minor wind acceleration phenomenon could be detected at ASU campus on ISTB4.
- Very mild wind acceleration happens on top of other high-rise buildings due to the effect of obstacle buildings at front. Which explains why the wind turbines mounted on top of Global Institute of Sustainability building are not working efficiently.

Chapter 4

CFD SIMULATION IN PHOENIX DOWNTOWN AREA

4.1 Introduction

This chapter focuses on the simulation of wind acceleration in Phoenix downtown area. As discussed in Chapter 2, no significant acceleration happens due to the lower altitude of buildings, so some relatively higher buildings are considered in this chapter to prove that energy at desperation point can make a difference to wind turbine performance.

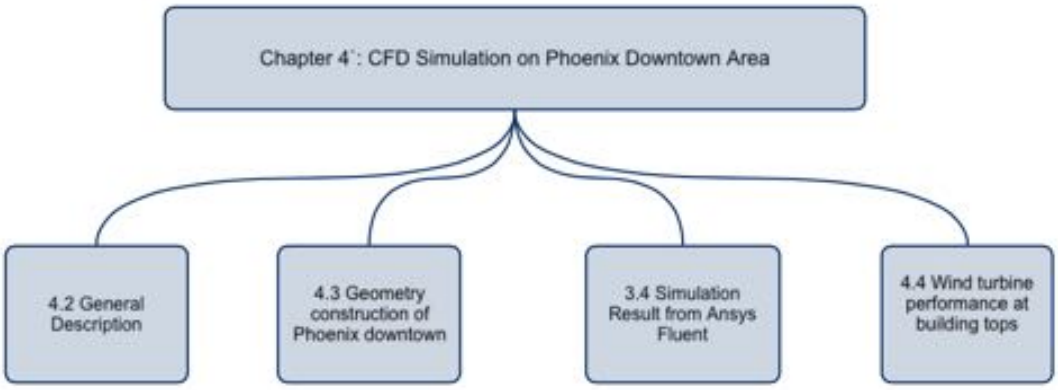

Figure 4.1: Chapter structure overview

4.2 General description

In the previous simulation on ASU campus, wind acceleration phenomenon is not significant due to the lack of high-rise buildings. To take advantage of energy from wind accelerations, wind turbine on higher buildings should be considered. This part of study has been performed for part of the Phoenix downtown 3D model with multiple skyscrapers.

There are a couple of successful cases with small wind turbine on high-rise buildings as mentioned in Chapter one. The main reason why turbines are installed on these buildings is that

higher buildings are less likely to be blocked by other geometries around and a steady high velocity can be gained all year around.

As it is less likely to install solar panels on high-rise buildings considering the maintenance cost and impact from high wind speed on rood tops. The wind turbines become a ideal source to provide clean sustainable energies.

4.3 Geometry construction of Phoenix downtown

Downtown Phoenix resembles a combination of multiple high-rise and flat buildings, where most of these higher buildings stand between Van Buren Street and Jackson Street, all the building above 35 m is marked in the Google map shown below:

Figure 4.2: Satellite map of a corner of ASU campus. This area contains a high density of high-rise buildings

There are multiple methods to change a 2D map into 3D geometry, as 3D GIS data of Phoenix downtown is unavailable from ASU library, it is impossible to build the geometry as in Chapter 3

for ASU campus model. In is study the geometry is constructed manually in Autodesk Inventor. The building structure and heights of PHX buildings are gained from online sources (Skyscraperpage.com). The highest buildings are listed in Fig 4.3.

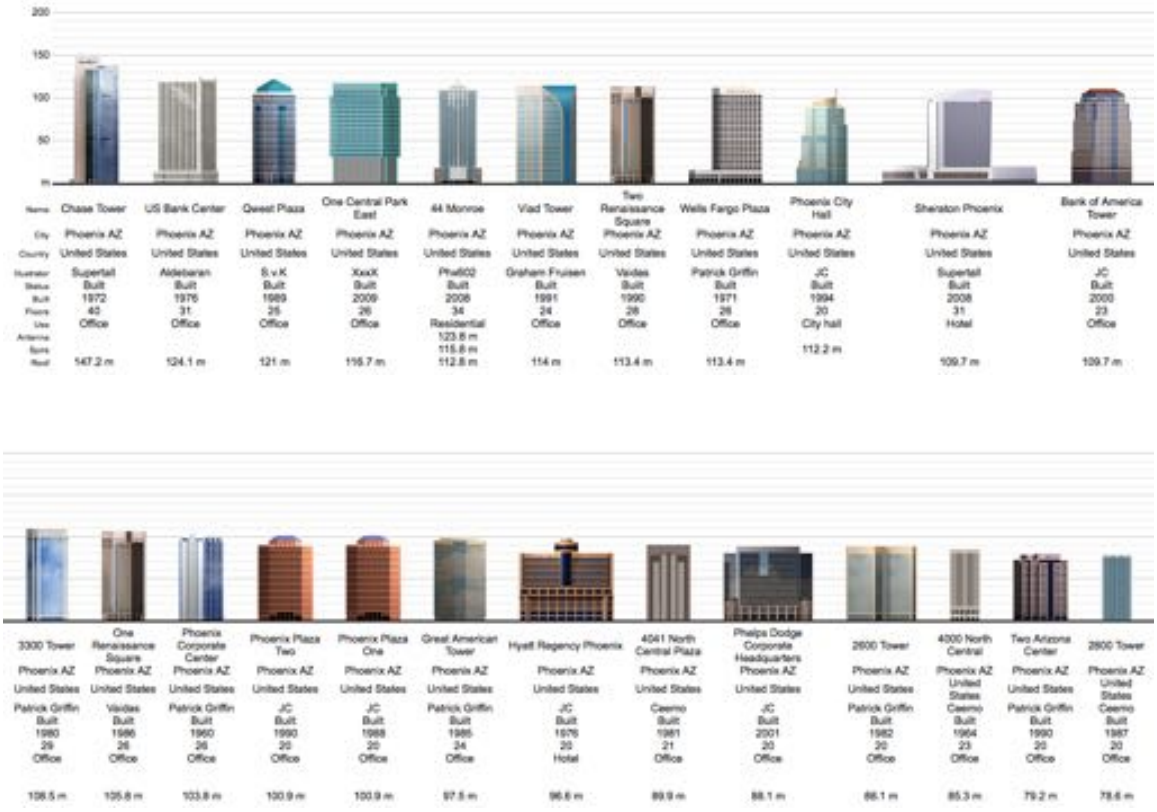

Figure 4.3: Phoenix skyscraper diagram with buildings higher than 75 m. 3D model is built based on this diagram

To prevent long simulation hours due to over detailed geometries, the buildings structure are simplified using the same method in Chapter 2 for ASU campus model. Buildings over 35 m in the region is marked out and detailed structure is obtained from the website. The final geometry is reconstructed in Autodesk Inventor is as below, where the highest building is measured as 147.2 m and lowest as 70 m:

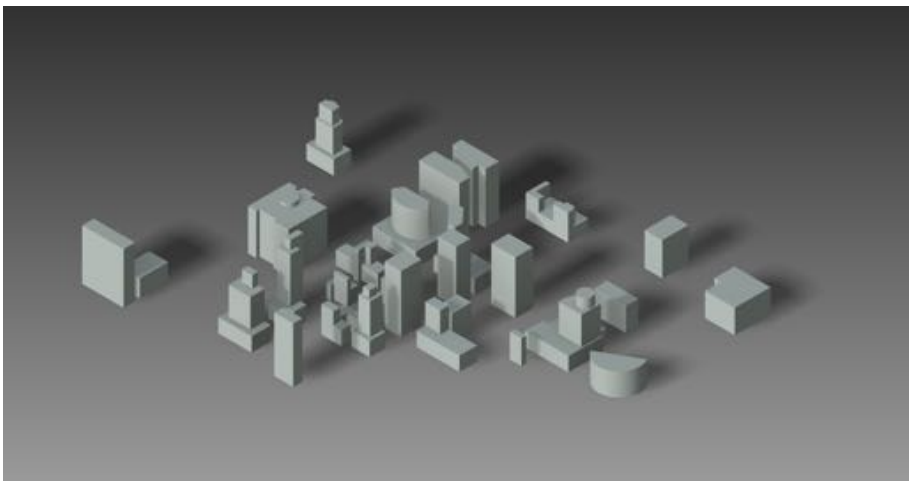

Figure 4.4: Phoenix skyscraper model built in Autodesk Inventor according to height and geometry data above

4.4 Simulation results from Fluent

A series of 3D simulations have been carried out with commercial software Ansys Fluent on the model built in section 4.2. Several slice plane were set across the simulation domain as in Fig. .

Phoenix downtown simulation domain

Phoenix downtown simulation plane of interest

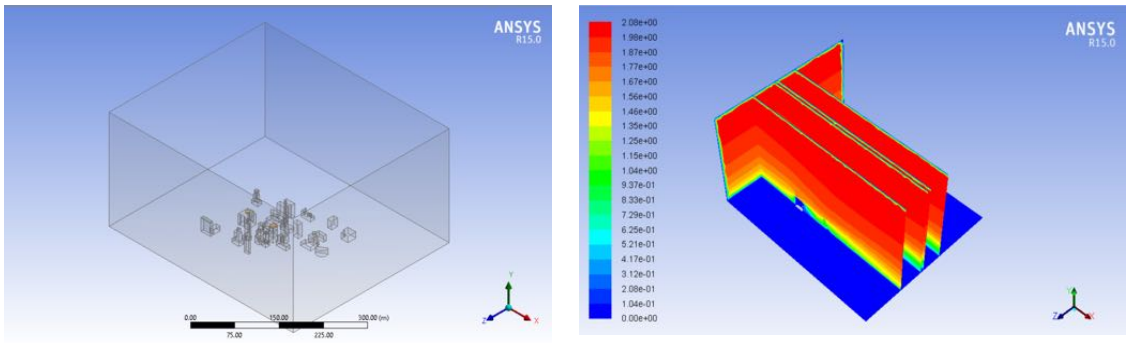

Figure 4.5: Phoenix skyscraper model numerical simulation domain (left) and slice planes placed crossed the buildings as in figure (right).

Phoenix case meshes – vertical plane

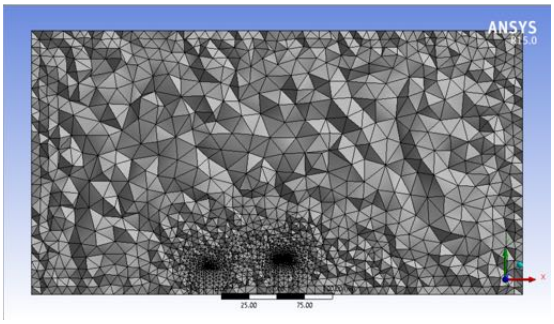

Phoenix case meshes – vertical plane (zoom-in)

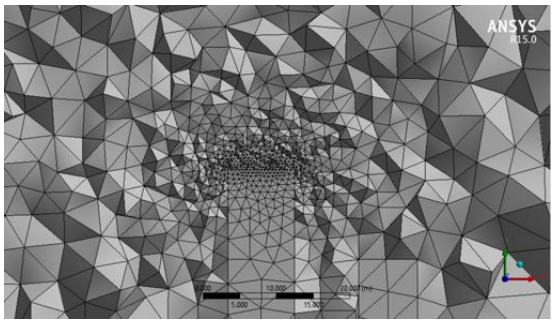

Figure 4.5: Phoenix skyscraper model mesh results on the whole vertical plane (left) and zoom-in mesh result (right)

A view of part of the meshed borders for the computational domain is obtained from the same mesh method in Chapter 2. The regions on several building tops are refined to finer meshes. The total nodes number is 92,276 and elements number is 510,071. The mesh gives an edge resolution of 0.8282 m.

The case is tested under three velocity inlet profiles from Chapter 2. As there is no available wind data near the geometry of interest, inlet velocity profile is calculated based on observation data is from Tempe Town Lake Weather Station, which is distant from Phoenix Downtown Area, the atmospheric boundary layer may not be very accurate. However, at this level of simulation, the main interest lies in the wind acceleration phenomenon and approximates location of highest velocity, it is not ideal be still acceptable to chose a wind profile like this.

The velocity magnitude contour on the four selected planes under medium velocity inlet are plotted and zoomed-in to determine whether there are visible accelerations happening on building tops.

Velocity magnitude contour – plane 1

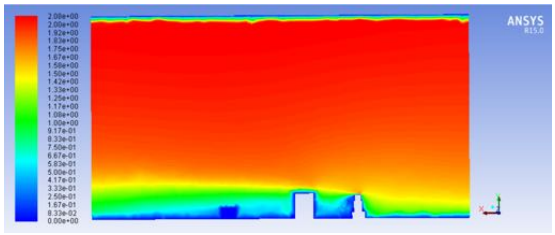

Velocity magnitude contour – plane 1 (zoom-in)

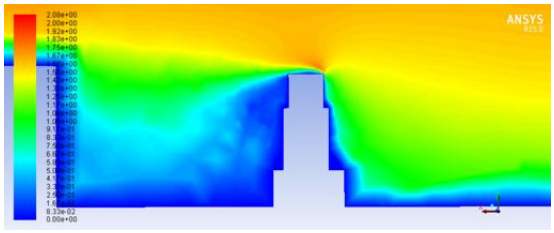

Velocity magnitude contour – plane 2

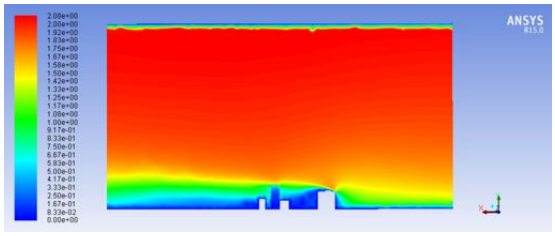

Velocity magnitude contour – plane 2 (zoom-in)

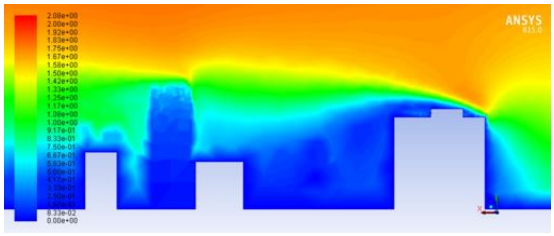

Velocity magnitude contour – plane 3

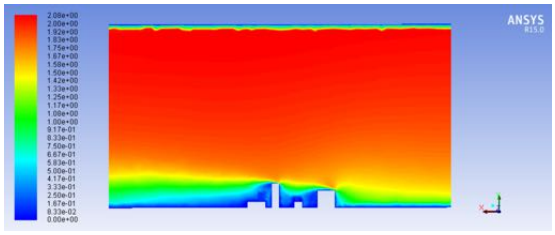

Velocity magnitude contour – plane 3 (zoom-in)

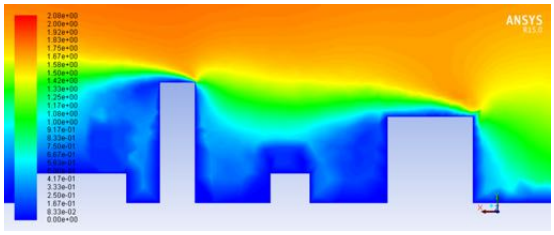

Velocity magnitude contour – plane 4

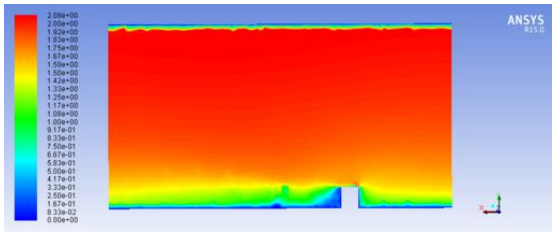

Velocity magnitude contour – plane 4 (zoom-in)

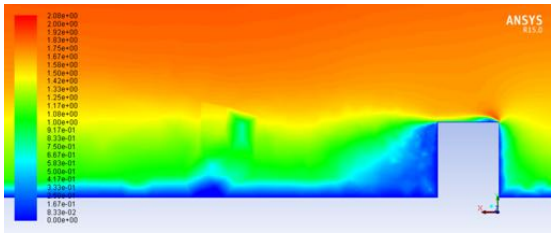

Figure 4.6: Phoenix skyscraper model velocity magnitude simulation results with medium velocity on the whole vertical plane (left) and zoom-in result (right)

As shown in the contours, there are significant wind accelerations on top of some buildings even when there are obstacle buildings between the building of interest and velocity

inlet. For the high velocity inlet case, the velocity contours are also plotted regarding the four slices planes. In the high velocity inlet condition, the velocity acceleration on building tops is even stronger, which indicates that, the stronger the wind is at the urban area boundary, the more acceleration it will cause on top of buildings. And there are more potential for the installation of rooftop small wind turbines.

Velocity magnitude contour – plane 1

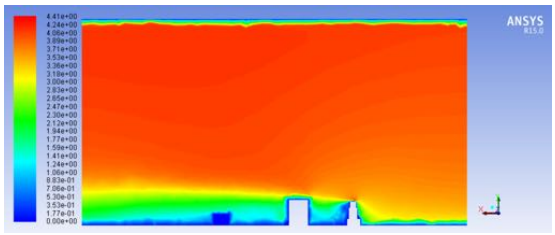

Velocity magnitude contour – plane 1 (zoom-in)

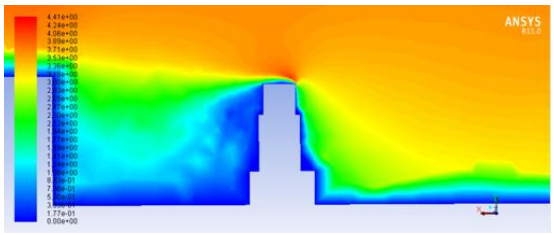

Velocity magnitude contour – plane 2

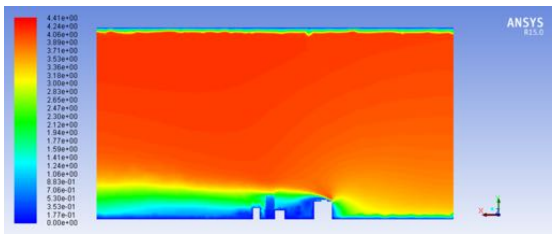

Velocity magnitude contour – plane 2 (zoom-in)

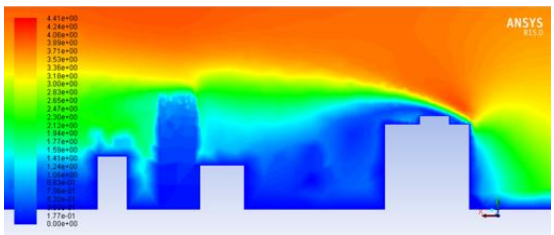

Velocity magnitude contour – plane 3

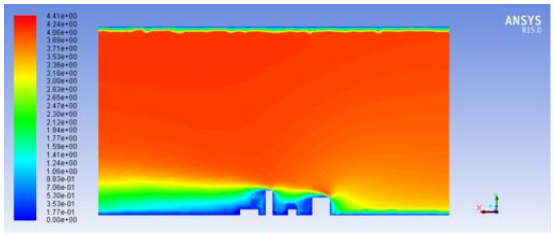

Velocity magnitude contour – plane 3 (zoom-in)

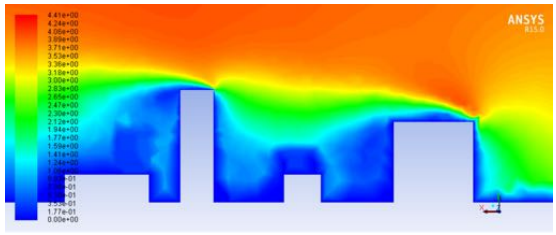

Velocity magnitude contour – plane 4

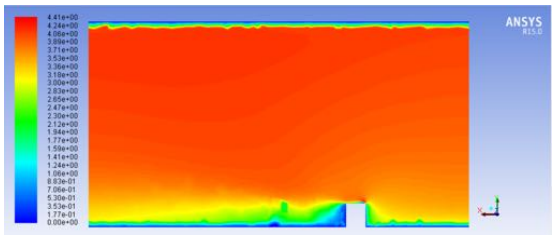

Velocity magnitude contour – plane 4 (zoom-in)

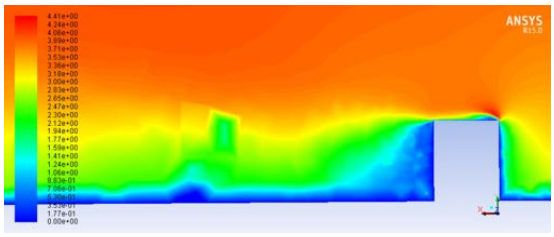

Figure 4.7: Phoenix skyscraper model velocity magnitude simulation results with high velocity at boundary on the whole vertical plane (left) and zoom-in result (right)

The velocity magnitude near corner of Sheraton Phoenix Downtown Hotel is highlighted in Fig 4.8. For the low inlet velocity case, where minor or even no acceleration could be detected in ASU campus model, the wind acceleration is not significant but still visible.

Velocity magnitude contour at low velocity (filled)

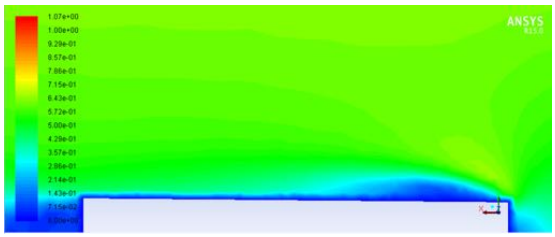

Velocity magnitude contour (not filled + line of interest)

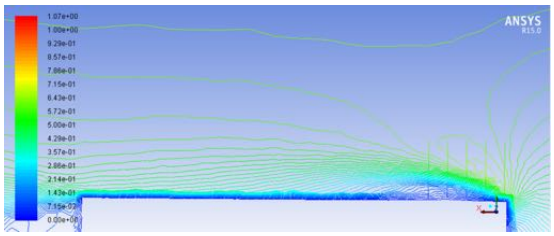

Velocity magnitude plots – detailed geometry

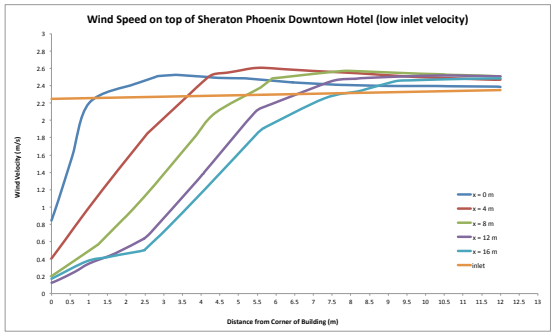

Velocity magnitude plots – acceleration ratio

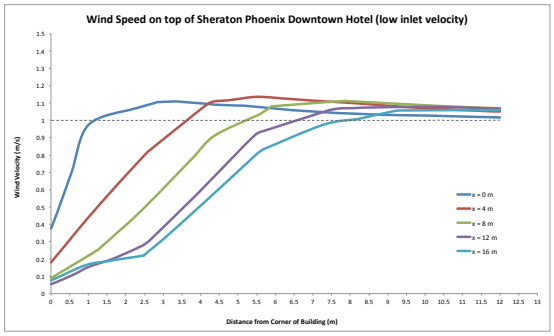

Figure 4.8: Velocity magnitude contours and plots with low velocity inlet boundary condition. The

acceleration phenomenon is not significant but still more visible compare to the velocity at ASU

Velocity at x = 0 m offset exceeds inlet velocity at same altitude the first at and velocity at x = 4 m offset reaches the greatest acceleration later at as in Fig 4.8 (c) and (d).

For the medium and high velocity inlet case, the acceleration phenomenon is similar to low inlet case but stronger emergence can be detected. The maximum acceleration happens at 2.5-3.5 m above building top at x = 0 m offset, which appears to be the best location for wind turbine installment.

Velocity magnitude contour – medium velocity

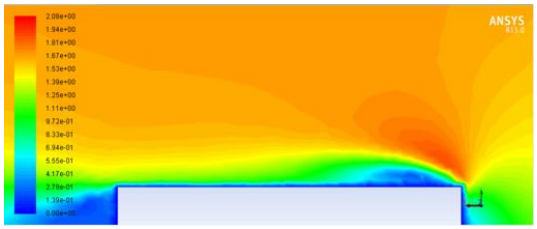

Line of interest – medium velocity

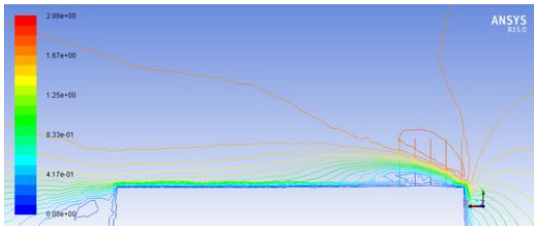

Velocity magnitude plots – medium velocity

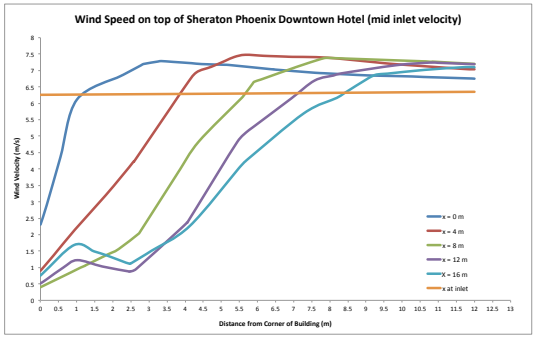

Acceleration ratio plots – medium velocity

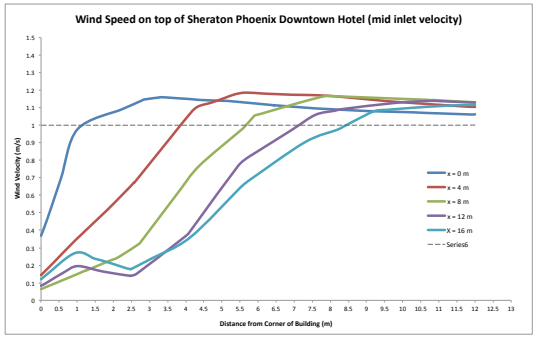

Velocity magnitude contour – high velocity

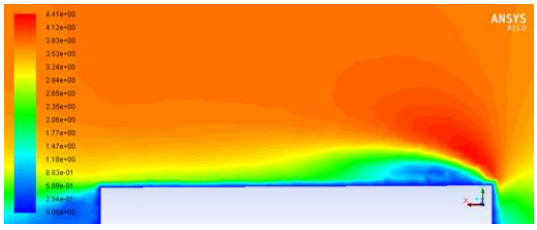

Line of interest – high velocity

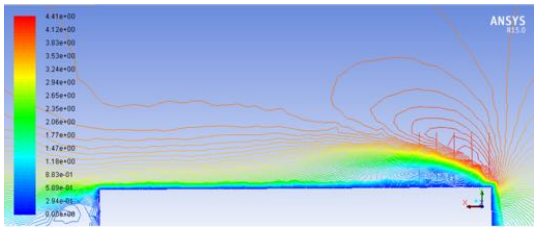

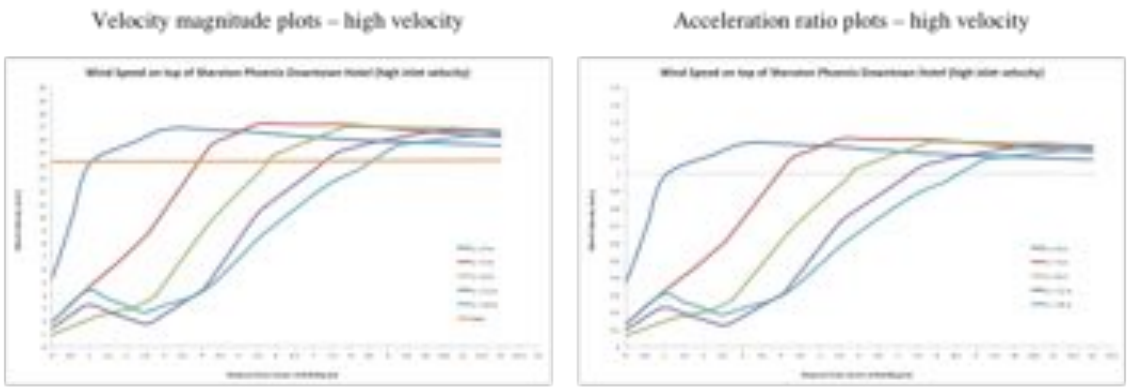

Figure 4.9: Velocity magnitude contours and plots with medium and high velocity inlet boundary

4.4 Wind turbine performance at building tops

Results from CFD simulations reveal the locations at zero offsets 2.5-3.5 m above rooftop are likely to be optimal for a roof-mounted wind turbine installation. To compare the wind turbine performance with and without acceleration affects, Honeywell Windgate RT6500 wind turbine is chosen and power production distribution is calculated on the Swiss Wind Power Data Website (Wind-data.ch). This wind turbine is a horizontal axis turbine with 1.7 meters diameter and approximately 20 blades, thus results in a low frictional resistance to rotate, making it possible for the turbine to have a cut-in speed close to 1 m/s. The power curve is plotted according to data obtained from the advertising pamphlet (Freepowerwindturbines.com).

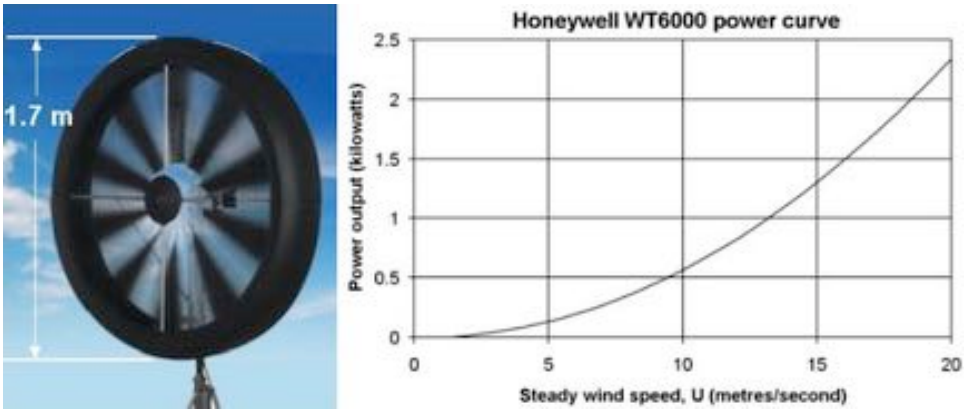

Figure 4.10: Honeywell WT6000 wind turbine demonstration picture and power performance curve

Weibull distribution at 3 m above building top is obtained with mean velocity and velocity range from previous simulations, using the same Weibull form parameter k as form Tempe Town Lake observation data.

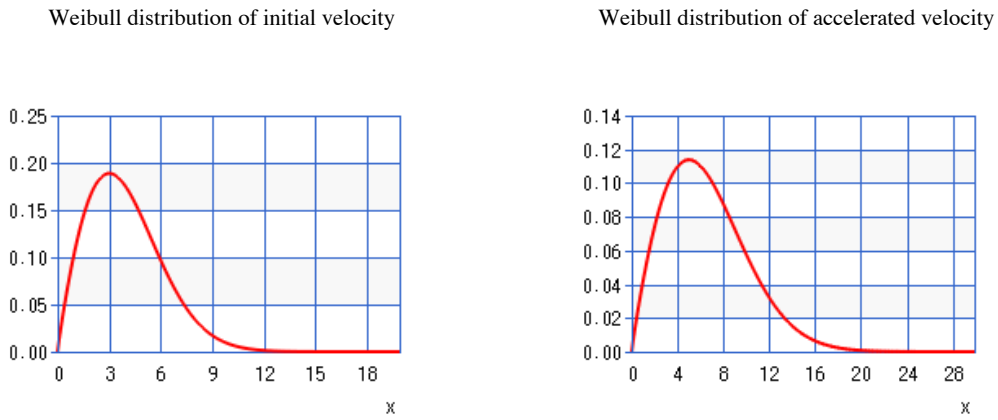

Figure 4.11: Weibull distribution of annual wind velocity at boundary and highest wind acceleration location on building top

The approximate power production result can be calculated based on turbine curve and wind distributions. Power production of wind turbine installed at observation center and on building top acceleration zone are listed as below.

Table 4.1: Wind turbine performance data at two different locations

Parameters	10 m above ground	Building Top
Capacity (kW)	5	5
Rotor Diameter (m)	1.7	1.7
Power Production (kWh/year)	929	3,534
Capacity Factor	2.2%	8.6%
Full Load Hours[2] (h/year)	197	749
Operating Hours[3] (h/year)	7,891	8,423

Results from table above is plotted as below:

Turbine performance – initial

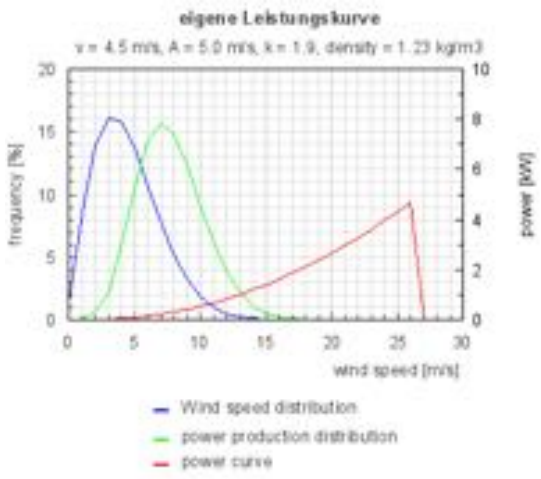

Turbine performance - accelerated

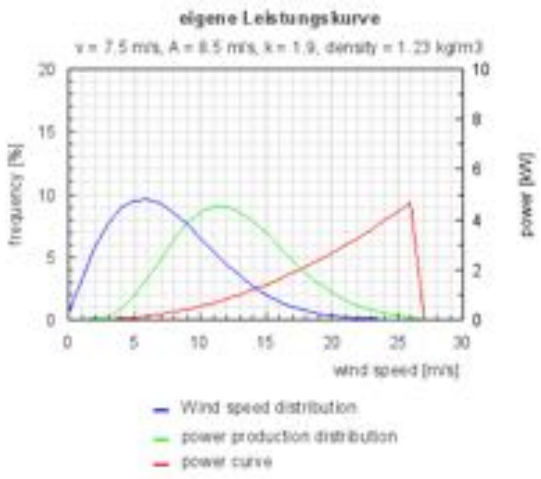

Figure 4.12: Wind turbine performance curve at two different locations

It can be concluded from the calculation results that roof-mount of Honeywell wind turbine brings 70% increase in power generations, which indicates that higher wind turbine power production could be accomplished by putting the turbine at correct place on roofs.

4.5 Conclusion

Wind acceleration in Phoenix downtown area was discussed in this chapter. Significant acceleration is detected and feasibility of using this acceleration for power generation is demonstrated.

It can be concluded that the acceleration of wind is strongly dependent on the structure and height of the buildings. For geometry involving high-rise building as this case, Best location for mounting the wind turbine can be determined by CFD simulations.

CHAPTER 5

CONCLUSIONS AND RECOMMENDATIONS FOR FUTURE WORK

5.1 Introduction

The content of this thesis focuses on using RANS computational fluid dynamics approach to simulate wind acceleration phenomenon in two complex geometries, ASU campus and Phoenix downtown. Additionally, acceleration ratio and locations are predicted, the results are then used to calculate the best location for small wind turbine installments. This chapter will recap the major findings relating to the CFD methods investigated and comment more broadly on how urban CFD simulation can be used as a reference method for future wind energy development.

5.2 Conclusions

There are two primary objectives in this work. First, perform CFD simulation on ASU campus and Phoenix downtown geometry to observe wind velocity changes on rooftops. Secondly, discuss the possibility of installing wind turbines on building tops that make good use of the acceleration phenomenon.

5.2.1 Local wind energy generation prediction

Several conclusions can be drawn from the simulations performed.

- The wind energy generated by wind turbine installed on rooftops can produce more energy comparing to the turbine 10 m above ground.
- Acceleration of wind velocity at separation zone is decided by velocity at inlet and building models.
- There are certain locations that can maximize local wind velocity, locations varies based on different geometries of interest. Which makes running case based CFD simulation before wind turbine installation very important.

5.2.2 CFD as a tool for assessing urban wind flow

It can be concluded that the CFD is the most relevant wind assessment tool for the purpose of integrating wind turbines within the built environment and assessing urban wind flow especially when the tool is used for comparing alternatives. However, CFD should be used vigilantly as it is embedded with errors and uncertainties. Thus, best practice guidelines should be consulted before using CFD as a simulation technique. However, it should be noted that these guidelines are not enough for having confidence in the yielded results. As the velocity inlet at boundaries is defined based on observation data, with more wind station involved in the simulation, a more accurate wind velocity profile can be predicted.

5.3 Recommendations for future works

This work contributes to understanding urban wind flow and wind flow around buildings, specifically around different real-life geometries for the purpose of mounting wind turbines.

Further analysis can be performed using ICEM meshing software for higher quality meshes and in-situ measurement of wind acceleration on the geometry of interest can act as an important validation procedure for the simulation. All of these works above have been mentioned and tested by previous researchers. However, it should be noted that wind turbine installation is not the only field that CFD simulation of ABL could be used.

Recently, there are growing concern about wind-related failures of solar panels installed on rooftops, these failures will be due, in part, to the lack of good information about wind loads on various kinds of solar collectors.

As shown in images below, for Phoenix downtown buildings in Fig... Wind accelerates greatly on building tops and great pressure difference can be detected across the first solar panel facing inlet velocity. Which means it is highly likely that the solar panels be peeled of from building tops.

Velocity contour – Phoenix downtown

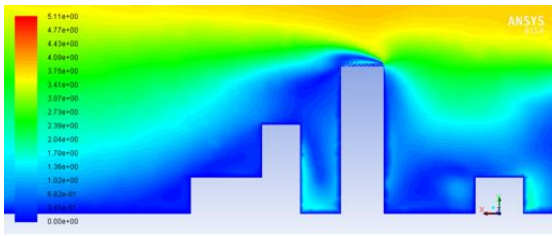

Velocity contour – solar panel (zoom in)

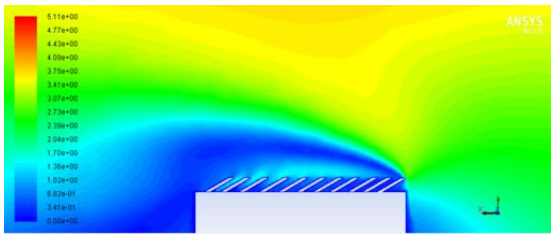

Pressure distribution contour – Phoenix city solar panel

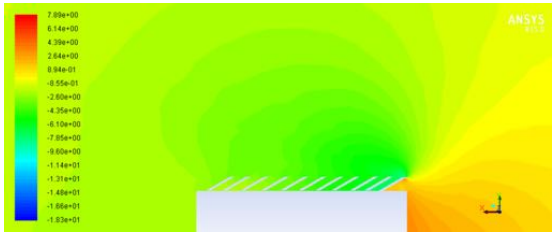

Turbulence intensity – Phoenix city solar panel

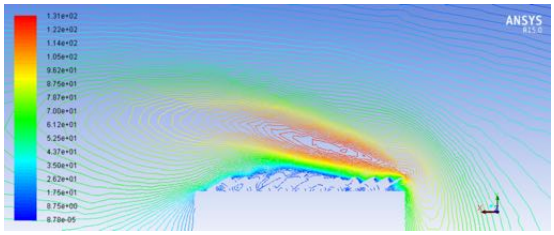

Figure 5.1: Wind profile distributions with solar panels installed on Phoenix downtown building. The contours show great pressure and velocity difference on the first solar panel facing wind

Velocity contour – ASU campus

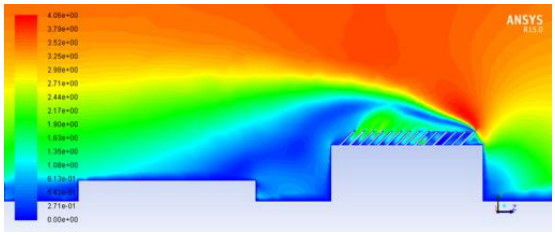

Velocity contour – solar panel (zoom in)

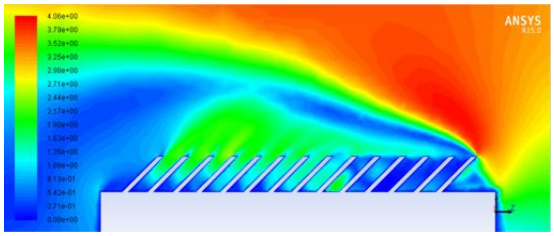

Pressure distribution contour – ASU campus solar panel

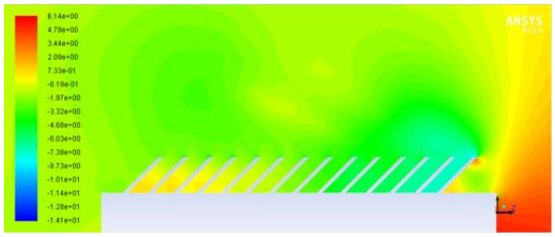

Turbulence intensity – ASU campus solar panel

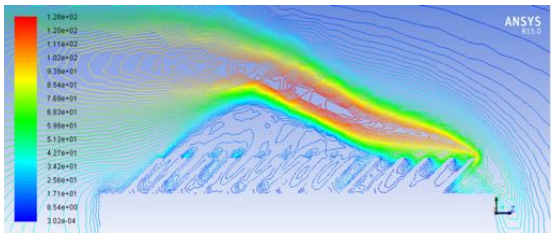

Figure 5.2: Wind profile distributions with solar panels installed on top of building at ASU campus. The pressure difference is not as significant as in Phoenix downtown case

Considering wind acceleration effects may also be helpful in preventing the failure of poorly installed solar panels.

5.4 Conclusion

Urban wind turbines is a relatively new field which is developing and has high potentials thanks to advancements in small and micro scale wind turbines technologies and the continues investigation of taking advantage of the accelerating effect of different buildings' shapes. This thesis goes some way towards addressing the developing wind turbines technologies to be integrated within buildings in addition to investigating the accelerating effect of different roof shapes. Overall, this thesis has striven to present a realistic and informative application of CFD to scalar dispersion in urban environments through investigation of a range of scales and modeling techniques.

REFERENCES

Burger, Bruno. 'Fraunhofer Institute for Solar Energy Systems ISE'. *Electricity Production From Solar And Wind In Germany*. Freiburg, Germany: Fraunhofer Institute for Solar Energy Systems ISE, 2015. 14. Web. 2 Apr. 2015.

Boxwell, Michael. *Solar Electricity Handbook*. Ryton on Dunsmore, Warwickshire, U.K.: Greenstream Pub., 2011. Print.

Abohela, Islam, Neveen Hamza, and Steven Dudek. 'Effect Of Roof Shape, Wind Direction, Building Height And Urban Configuration On The Energy Yield And Positioning Of Roof Mounted Wind Turbines'. *Renewable Energy* 50 (2013): 1106-1118. Web.

Bazrafshan, Jafar et al. 'CFD Calculation Of Wind Turbines Power Variations In Urban Areas'. *AMR* 622-623 (2012): 1084-1088. Web.

Blocken, B., and J. Persoon. 'Pedestrian Wind Comfort Around A Large Football Stadium In An Urban Environment: CFD Simulation, Validation And Application Of The New Dutch Wind Nuisance Standard'. *Journal of Wind Engineering and Industrial Aerodynamics* 97.5-6 (2009): 255-270. Web.

Blocken, B., and J. Persoon. 'Pedestrian Wind Comfort Around A Large Football Stadium In An Urban Environment: CFD Simulation, Validation And Application Of The New Dutch Wind Nuisance Standard'. *Journal of Wind Engineering and Industrial Aerodynamics* 97.5-6 (2009): 255-270. Web.

Jie, Yin et al. 'Correlation Between Urban Morphology And Wind Environment In Digital City Using GIS And CFD Simulations'. *Int. J. Onl. Eng.* 10.3 (2014): 42. Web.

Ai, Z.T., and C.M. Mak. 'Large Eddy Simulation Of Wind-Induced Interunit Dispersion Around Multistory Buildings'. *Indoor Air* (2015): n/a-n/a. Web.

Lettau, H. 'Note On Aerodynamic Roughness-Parameter Estimation On The Basis Of Roughness-Element Description'. *J. Appl. Meteor.* 8.5 (1969): 828-832. Web.

Anderson, John David. *A History Of Aerodynamics And Its Impact On Flying Machines*. Cambridge [u.a.]: Cambridge Univ. Press, 1997. Print.

Kauffman, Joanne, and Kun-Mo Lee. *Handbook Of Sustainable Engineering*. Dordrecht: Springer, 2013. Print.

Bhattacharya, Paritosh, and Rakhi Bhattacharjee. 'A Study On Weibull Distribution For Estimating The Parameters'. *Wind Engineering* 33.5 (2009): 469-476. Web.

Wx.tempe.gov,. 'Town Lake Weather Monitor'. N.p., 2015. Web. 2 Apr. 2015.

Yeo, DongHun, and Emil Simiu. 'High-Rise Reinforced Concrete Structures: Database-Assisted Design For Wind'. *Journal of Structural Engineering* 137.11 (2011): 1340-1349. Web.

CASTRO, I P, and J M R GRAHAM. 'NUMERICAL WIND ENGINEERING: THE WAY AHEAD ?'. *Proceedings of the ICE - Structures and Buildings* 134.3 (1999): 275-277. Web.

Hu, C.-H. '*Proposed Guidelines of Using CFD and the Validity of the CFD Models in the Numerical Simulations of Wind Environments around Buildings*.' PhD thesis (2003), Heriot-Watt University.

Franke, Jorg et al. 'The COST 732 Best Practice Guideline For CFD Simulation Of Flows In The Urban Environment: A Summary'. *International Journal of Environment and Pollution* 44.1/2/3/4 (2011): 419. Web.

Crasto, Giorgio. "Numerical simulations of the atmospheric boundary layer." PhD thesis (2007), *Università di Cagliari*.

Varghese, Sonu S., Steven H. Frankel, and Paul F. Fischer. 'Modeling Transition To Turbulence In Eccentric Stenotic Flows'. *Journal of Biomechanical Engineering* 130.1 (2008): 014503. Web.

Lei, Li et al. 'Numerical Simulation Of The Flow Within And Over An Intersection Model With Reynolds-Averaged Navier–Stokes Method'. *Chinese Phys.* 15.1 (2006): 149-155. Web.

Mertens, Sander. 'Wind Energy In The Built Environment - Concentrator Effects Of Buildings'. *Wind Engineering* 30.5 (2006): 451-452. Web.

ASU Wind Turbines Generate Electricity and Interest,. 'Institute News / Global Institute Of Sustainability / Arizona State University'. N.p., 2008. Web. 2 Apr. 2015.

Lib.asu.edu,. 'ASU GIS Data Repository | ASU Libraries'. N.p., 2015. Web. 2 Apr. 2015.

Asu.edu,. 'ASU Interactive Map'. N.p., 2015. Web. 2 Apr. 2015.

Hall, R.C. (Ed.), *Evaluation of modelling uncertainty. CFD modelling of near-field at- mospheric dispersion. Project EMU final report*, 1997. Print

Tominaga, Yoshihide et al. 'AIJ Guidelines For Practical Applications Of CFD To Pedestrian Wind Environment Around Buildings'. *Journal of Wind Engineering and Industrial Aerodynamics* 96.10-11 (2008): 1749-1761. Web.

VirginiaTech ARC,. '5.2.2. Mesh Quality'. N.p., 2015. Web. 2 Apr. 2015.

Bern, Marshall, David Eppstein, and John Gilbert. 'Provably Good Mesh Generation'. *Journal of Computer and System Sciences* 48.3 (1994): 384-409. Web.

Weerasuriya, A. U. 'Computational Fluid Dynamic (CFD) Simulation Of Flow Around Tall Buildings'. *Engineer: Journal of the Institution of Engineers, Sri Lanka* 46.3 (2014): n. pag. Web.

Menter, F. R. 'Two-Equation Eddy-Viscosity Turbulence Models For Engineering Applications'. *AIAA Journal* 32.8 (1994): 1598-1605. Web.

Van Hooff, T., B. Blocken, and M. van Harten. '3D CFD Simulations Of Wind Flow And Wind-Driven Rain Shelter In Sports Stadia: Influence Of Stadium Geometry'. *Building and Environment* 46.1 (2011): 22-37. Web.

Blocken, Bert, Ted Stathopoulos, and Jan Carmeliet. 'CFD Simulation Of The Atmospheric Boundary Layer: Wall Function Problems'. *Atmospheric Environment* 41.2 (2007): 238-252. Web.

Skyscraperpage.com,. 'Phoenix Skyscraper Diagram - Skyscraperpage.Com'. N.p., 2015. Web. 3 Apr. 2015.

Wind-data.ch,. 'Windenergie-Daten Der Schweiz'. N.p., 2015. Web. 3 Apr. 2015.

Freepowerwindturbines.com,. 'Wind Turbine Energy Systems Technology | West Michigan'. N.p., 2015. Web. 3 Apr. 2015.

APPENDIX A

UDF FUNCTION SCRIPT FOR U-WIND

UDF function script for u-wind are as below:

For the low velocity profile:

```
#include "udf.h"

DEFINE_PROFILE(x_velocity,thread,nv)

{
  real x[ND_ND];

  real y,z;

  face_t f;

  begin_f_loop(f, thread)

{
   F_CENTROID(x,f,thread);

    y = x[1];
    z = x[2];

   F_PROFILE(f, thread, nv) = .23325*log((y-1)/0.032)-1;
  }

  end_f_loop(f, thread)
}
```

For the medium velocity profile:

```
#include "udf.h"

DEFINE_PROFILE(x_velocity, thread, nv)

{
  real x[ND_ND];

  real y,z;

  face_t f;

  begin_f_loop(f, thread)

{
   F_CENTROID(x,f,thread);

    y = x[1];
    z = x[2];
```

```
  F_PROFILE(f, thread, nv) = 1.866*.125*log((y)/0.032);
 }

 end_f_loop(f, thread)
}
```

For the high velocity profile:

```
#include "udf.h"

DEFINE_PROFILE(x_velocity,thread,nv)

{
  real x[ND_ND];

  real y,z;

  face_t f;

  begin_f_loop(f, thread)

{
   F_CENTROID(x,f,thread);

    y = x[1];
    z = x[2];

   F_PROFILE(f, thread, nv) = 1.866*.125*log((y-1)/0.032)+2;
  }

  end_f_loop(f, thread)
}
```